EVALUATION OF THE PERFORMANCE OF GEOTEXTILE REINFORCED RED COFFEE SOIL EMBANKMENTS WITH SAND CUSHIONS SUBJECT TO RAINFALL EVENT

SALIM ALI ZIMBU

MASTER OF SCIENCE IN CIVIL ENGINEERING

(Structural Option)

PAN AFRICAN UNIVERSITY

INSTITUTE FOR BASIC SCIENCES, TECHNOLOGY AND INNOVATION

2018

Evaluation of the Performance of Geotextile Reinforced Red Coffee Soil Embankments with Sand Cushions Subject to Rainfall Event

Salim Ali Zimbu

CE300-0013/17

A thesis submitted to the Pan African University Institute for Basic Sciences, Technology and Innovation in partial fulfilment for the award of the Degree of Master of Science in Civil Engineering

2018

DECLARATION

This thesis is my original work and has not been presented for a degree in any other University.

Signature: ---------- Date: ----------

Salim Ali Zimbu

CE300-0013/17

This thesis has been submitted with our approval as the university supervisors.

Signature: ---------- Date: ----------

Dr Joseph N. Thuo, PhD

DeKUT, Kenya

Signature: ---------- Date: ----------

Dr Nathaniel O. Ambassah, PhD

JKUAT, Kenya

DEDICATION

To my family for the love, encouragement and support.

ACKNOWLEDGEMENT

First and foremost I would like to thank the Almighty Allah for the gift of life and health without which this work would not have been possible. I also wish to express my heartfelt gratitude to my supervisors, Dr Joseph Thuo and Dr Nathaniel Ambassah for their expertise guidance, valid comments, suggestions, continuous support and untiring efforts in carrying out this project.

I would also like to extend my sincere gratitude to the Pan Africa University Institute for Basic Sciences, Technology and Innovation for providing me with the platform to undergo my postgraduate studies. Much appreciation to all my colleagues who positively contributed to the success of this work.

TABLE OF CONTENTS

LIST OF FIGURES

LIST OF TABLES

LIST OF ABBREVIATIONS AND ACRONYMS

AASHTO	American Association of State Highway and Transportation Officials
AEV	Air Entry Value
ASTM	American Society for Testing and Materials
FEM	Finite Element Method
FHWA	Federal Highway Administration
FOS	Factor of Safety
GRS	Geosynthetic Reinforced Soils
LEM	Limit Equilibrium Method
MSE	Mechanically Stabilised Earth
PWP	Pore-water Pressure
PWRI	Public Works Research Institute of Japan
RCS	Red Coffee soils
SWCC	Soil Water Characteristic Curves
USCS	Unified Soil Classification System
WEV	Water Entry Value
WRC	Water Retention Curve

ABSTRACT

Geosynthetic reinforced soil (GRS) structures are in a period of enormous growth in Kenya's infrastructure projects. This is due to their numerous advantages over conventional retaining structures which include improved stability and reduced base area in the construction of the structures. However, economic and environmental constrains have necessitated the use of locally available fine grained soils as backfill material contrary to design guidelines recommendations. The guidelines provide that backfill material should be non-cohesive sand. The main deterrent in the use of fine grained soil as backfill material is its inability to quickly drain water, leading to build up of pore-water pressures. The use of nonwoven geotextile drains within these backfills has been suggested in the reduction of the pore water pressure. However, it is recognized that the nonwoven geotextile retard water due to capillary barrier effect under unsaturated soil conditions and start to act as a drainage material only when the soil immediately above it became nearly saturated. The aim of this study was to evaluate the performance of red coffee soils embankments when incorporated with sand layers to aid in drainage. Specifically the study evaluated the effect of inclining non-woven geotextile layers on the performance of red coffee soils embankments, it evaluated the effect of the sand layer thickness on the performance of the red coffee soils embankments and looked into the effect of drainage layers spacing on the performance of the red coffee soils embankments. The numerical model SEEP/W that employs the use of the elliptical transient Richard's equation was adopted in the analysis of infiltration into the unsaturated soil backfill while the Spencer method; a limit equilibrium method of slope stability analysis in SLOPE/W was used in evaluating the stability of the embankments. Findings from the numerical study showed that non-woven geotextile became more effective in drainage when inclined at 3° above the horizontal in red coffee soils embankments. Sand cushion layers improved both the drainage and stability of the red coffee soils embankment in long term rainfall events. It was concluded that sand layers can be safely used to improve on the drainage and stability red coffee soils embankments subject to long duration rainfall events.

CHAPTER ONE

INTRODUCTION

1.1 Background

Over the last two decades Kenya has experienced enormous growth in infrastructure such as railway tracks, highways, dams, irrigation canals, and buildings. The construction of these infrastructure comes along with the need for embankments. For example in the construction of the highways, embankments have been developed in area of interchanges, the Standard Gauge Railways has incorporated the use of embankments in most sections. This brings about the need for safety and economics in ensuring the stability of these embankments. In order to guarantee stability of cut or fill slopes, the use of geosynthetic reinforcements has been adopted. Geosynthetic reinforcement is a polymeric material composed of either polyester, polyethylene or polypropylene which is manufactured into geotextile or geogrid. The reinforcement provides tensile capacity to the soils and enables a soil slope to be retained at angles steeper than the materials angle of repose (Shukla, Sivakugan, & Das, 2011).

There has been a rapid development of geosynthetics reinforced structures all over the world owing to number of factors including low cost, aesthetics, reliability, simple construction techniques, and the ability of the reinforced soil structures to adapt to different site conditions (Raisinghani & Viswanadham, 2011). Many successful geosynthetic reinforced soil (GRS) structures provide the strong evidence for its advantages; however, there has been an increase in the number of GRS failures. Factors attributing to reinforced slope failures can be divided into natural and man-

made factors (Wu, Chou, & Tang, 2010). Natural factors include rainfall characteristics and earthquakes while human activities are inadequate planning, erroneous analysis and design, unqualified material, poor construction, improper serve and maintenance.

Many researches (Koerner & Koerner, 2013; Wu et al., 2010) reported that intense rainfall and low quality of backfill have been the main factors responsible for reinforced slope failures. Wu et al., (2010) indicated that about 89.47% of the failures he investigated were related to the intense rainfall and about 31.58% of the failures were caused by the poor quality of backfill material. Koerner & Koerner, (2013), reported that 61% of the failed slope cases had used silt and/ or clay as backfill and 60% of the failure cases were caused by internal or external water.

1.2 Problem Statement

Generally, cohesionless soils are prefered as backfills for GRS structure due to their high soil shear strength, interface shear strength and good drainage ability as recommended in AASHTO,(2002) ; FHWA, (2009). However, in many construction sites economic benefits of GRS have often been prohibitive owing to cost of recommended granular backfill and transportation costs of such backfill materials. A study by Raisinghani et al., (2011) reported that backfill materials forms one of the major constituent of a geosynthetic reinforced soil wall and slope and accounts for around 30-40% of their cost.

In addition, there is environmental concerns related to disposal of locally available soils and excavation of new granular materials from borrow pits and river valleys. Patricia, (2015), reported that sand harvesting along rivers has contributed to the

destruction of river banks and drained water points leading to drying of rivers. Rivers are a source of livelihood for human and other living creatures and destruction of such features directly affects them.

Different soils are available in various parts of the country as a results of cuts to give the required formation levels in construction. Red coffee soils can be cheaply sourced in most parts of Kenya as they form part of waste material in most construction areas. However, design guidelines (FHWA, 2009; AASHTO, 2002) limits the use of fine-grained soils(termed as marginal fills) within the reinforced zone. The main challenge in the use of marginal fills is the uncertainty of pore-water pressure (PWP) variations within the reinforced zones subjected to various moisture conditions. Studies have suggested that efforts to improve on the drainage of marginal fills can make them useful as backfill materials in embankments and slopes (Berg et al., 2009).

From the previous studies the quality of the backfill material, extreme rainfall exposure and type of geosynthetic materials has been found to have a major influence on the functionality of GRS slopes. A study on the performance of locally available marginal soils when used in geosynthetics reinforced slopes is therefore necessary. This study thus aims to evaluate the potential of RCS as a backfill material in the construction of embankments. Sand cushions have been suggested in the improvement of drainage and stability of the RCS embankments when subjected to rainfall event.

1.3 Objectives

1.3.1 General objectives

To evaluate the performance of reinforced RCS embankments with sand cushions subject to rainfall event

1.3.2 Specific objectives

The specific objectives of this study are:

i. To model infiltration in unsaturated soils backfill using SEEP/W

ii. To assess effect of non-woven geotextile layers inclination on the drainage and stability of red coffee soil embankments

iii. To evaluate the effect of sand cushion thickness on drainage and stability of red coffee soil embankment

iv. To assess effect of drainage layers spacing on the drainage and stability of red coffee soil embankments

1.4 Justification of the Study.

There is great need to ensure sustainability in construction projects. Sustainability has three main dimensions which include economical, ecological and social sustainability. The use of marginal soils as backfill in construction is going to positively address the ecological sustainability issues. In considering the ecological sustainability, emphasis is on the reuse of materials and reduction of waste. The use of marginal soils as backfill will reduce the amount of CO_2 emissions and energy requirements necessary in the extraction and transportation of new material from the quarries. This will by an extent

reduce the pollution of lands due to damping of the excavated materials to sites which would have otherwise been of economic benefits. Economic sustainability will be achieved as a cheaper source of backfill material will now be available. Christopher & Stulgis,(2005) reports that marginal backfill have the potential of reducing backfill cost to a third.

Findings of this study will thus lead to a safe use of locally available red-coffee soil as backfill material in geosynthetic reinforced structures through

i. Developing improved methodologies for the design of reinforced soil structures constructed with locally available soils and

ii. Providing a suitable guidance of selecting an appropriate drainage system for a reinforced red-coffee soil slope.

These findings will lead to economical GRS structures through reduction of transportation cost of backfill materials. It will contribute to environmental conservation due to reduction of quantities of disposed locally available cut material as witnessed in the current construction practices as well as minimise the mining of granular materials which leave ugly scars on the earth surface and in cases pose a threat to the existence of rivers.

1.5 Scope of the Study

This study developed numerical models using the GeoStudio software and validated it for its accuracy in infiltration analyses as well as its suitability for stability analyses using the laboratory tests results of RCS. Basic geotechnical characterization of RCS

and cushion materials were done in the PAUISTI and JKUAT laboratories. Finally, series of numerical experiment were conducted and discussed.

CHAPTER TWO

LITERATURE REVIEW

2.1 Introduction

This chapter presents the theoretical and empirical works done on the characteristics of unsaturated soils, moisture distribution in such soils and their shear strength. It reviews GRS structures and modelling of such structures using software and cases of failure of such structures. The introduction of sand cushion in GRS structures and their effect have also been reviewed.

2.2 Marginal Soils Backfill

The use of reinforced soils for the construction of retaining walls embankments slopes and in the stabilization of soft grounds has gained prominence in the recent years. Unlike in the past times where unreinforced slopes were common, reinforced embankments present a number of advantages as compared to unreinforced slopes. Reinforced embankments possess higher shear strength capacity and occupy much lesser space as compared to their unreinforced counterparts, they have also proven cost wise effective when compared to high retaining walls that may have been required in the case of embankments construction.

In the construction of these embankments the codes have recommended properties for the backfill materials to be used. According to AASHTO, (2002) and FHWA, (2009) the soils recommended as backfill need to be cohesionless soils due to their high soil shear strength, interface shear strength and good drainage ability. Properties of the soils to be adopted as recommended in the FHWA document are as summarised in the Table 2.1.

Table 2.1: Recommended backfill soil properties (FHWA, 2009)

	U.S. Sieve Size	**Percent passing**
Gradation (AASHTO T-27)	4 in. (102mm)	100
	No. 40 (0.425mm)	0-60
	No. 200(0.075mm)	0-15
Plasticity Index, PI (AASHTO T-90)	$PI \leq 6$	

Despite the recommendations, the use of marginal soils not meeting the recommended properties has been in practice. This can be attributed to the high cost required in the use of the compliant soils costs associated with extraction and transportation of these compliant soils (Thuo, Huynh, Yang, & Portelinha, 2016). Use of marginal soils has been reported in a number of studies including the review of GRS walls of North America as reported by Christopher et al., (2005) in which marginal soils had been used in the construction of GRS structures with a degree of success.

In this study RCS was evaluated in its performance as a backfill material in embankments. A number of studies have been conducted to determine the properties of the RCS of central Kenya. Researchers (Denge, 2017; Njike, Oyawa, & Nyomboi, 2014) have reported the properties of the RCS of Juja located in Central Kenya. They reported the RCS of Juja were predominantly silty clays with a specific gravity of 2.261. The RCS had a liquid limit of 25%, plastic limit of 25%, and a linear shrinkage of 17%. They further reported, from the compression laboratory test carried out the optimum moisture content of the RCS was 26.5% with a maximum dry density of 1327Kg/m^3.

From the previous studies from RCS is observed to have high plasticity index beyond the recommended 6% specified by the code (AASHTO, 2002). With such high

plasticity index and low hydraulic conductivity the safety of the embankments to be considered. The failure of reinforced structures such as walls and embankments is attributed to marginal soil backfills and rainfall infiltration.

Koerner et al., (2013) investigated the failure of 171 failed geosynthetic MSE walls. In the investigation they reported that 91% of the failed walls were geogrid reinforced, this was majorly attributed to the fact that despite geogrid layers providing reinforcement to the embankments they performed poorly in the dissipation of pore-water pressure within the embankments leading to eventual failure of the structures. 61% of the walls were composed of silt or clay backfill, the failure of 98% of the walls was attributed to improper design and 60% of the failures was attributed to internal or external water. In the report they attributed the failure generally to poor drainage procedures and development of hydraulic pressure within the marginal backfill soils.

Yoo et al., (2006) in another study investigated the failure of a segmental GRS wall in Korea after a monsoon season. The investigation revealed that the major contributor to the failure of the wall was largely attributed to fine-grained backfill and rainfall infiltration. For the proper functioning of these structures composed of marginal backfill, studies (Christopher & Stulgis, 2005; Garcia, Gallage, & Uchimura, 2007; Yang, Thuo, Huynh, Nguyen, & Portelinha, 2017) have proposed the need for proper drainage within these structures. The use of non-woven geotextile has been reported to aid in the improvement of the performance of walls and slopes composed of marginal backfills.

Tolooiyan et al., (2009) proposed when fine-grained soil is used as backfill, the use of nonwoven geotextile has to be considered to provide drainage. Nonwoven geotextile

was reported to have increase the stability of soil structure by providing both reinforcement and drainage function. Iryo et al., (2005) reported of non-woven geotextile materials with a saturated hydraulic conductivity of 0.023m/s which was significantly high compared to the hydraulic conductivity of marginal soils. In addition to drainage geotextile the layers provides a tensile capacity that helped increase the strength of the embankment, successfully improving the performance of the marginal embankments.

2.3 Numerical Modelling of Infiltration in Unsaturated Soils

With the advent of computers numerous analysis programs are available in the analysis of infiltration and stability of embankments and walls. Two basic approaches of analysis have been adopted; the limit equilibrium method and the finite element method (FEM). In the limit equilibrium method the approach includes the use of the basic equations of slices that are in use in the computation of stability of slopes. The approach tends to balance the moments and forces of slices in the circle of failure. On the other hand in the finite element analysis the stress- strain of the soils and constitutive laws are taken into consideration. SLOPE/W numerical model is one of the various limit equilibrium element based programs that is in use in the analysis. In SLOPE/W transient analysis a critical analysis in the evaluation of performances is incorporated.

2.3.1 Transient water flow in SEEP/W

Transient analysis is one in which the boundary conditions of the finite elements are a function of time. In SEEP/W a model developed by GeoSlope, the Richard's equation (1931) as shown in Equation 2.1 was integrated to govern transient water flow within

an unsaturated soil. For a two-dimensional homogenous anisotropic soil, the equation is derived as follows:

$$k_x \frac{\partial^2 h}{\partial x^2} + k_y \frac{\partial^2 h}{\partial y^2} = \frac{\partial \theta}{\partial t} = m_w \gamma_w \frac{\partial h}{\partial t} \quad \textbf{(2.1)}$$

Where;

h = total hydraulic head; k_x = unsaturated hydraulic conductivity in the x direction; k_y = unsaturated hydraulic conductivity in the y direction; m_w = coefficient of water volume change (slope of the water characteristics curve); γ_w = unit weight of water; θ = volumetric water content. The parameters m_w, k_x, *and* k_y are material specific, and are defined as function of pore pressure (Iryo & Rowe, 2003).

Before the application of the Richard's equation in the transient analysis, the water function of the geomaterial (i.e. sand, soil or geotextile) has to be described. Water retention curve are an important element in the transient analysis of infiltration in unsaturated geomaterial. It describes the relationship between the amount of water retained in a geomaterial and suction. They are constructed following two processes: the wetting and drying processes of the geomaterial. The amount of water can be measured by three common ways that are gravimetric water content (ω), volumetric water content (θ), and degree of saturation (S). Volumetric water content is defined as the ratio of volume of water to the total volume of soil as in Equation 2.2:

$$\theta = \frac{V_w}{V_T} \quad \textbf{(2.2)}$$

Figure 2.1 shows a schematic water retention curve

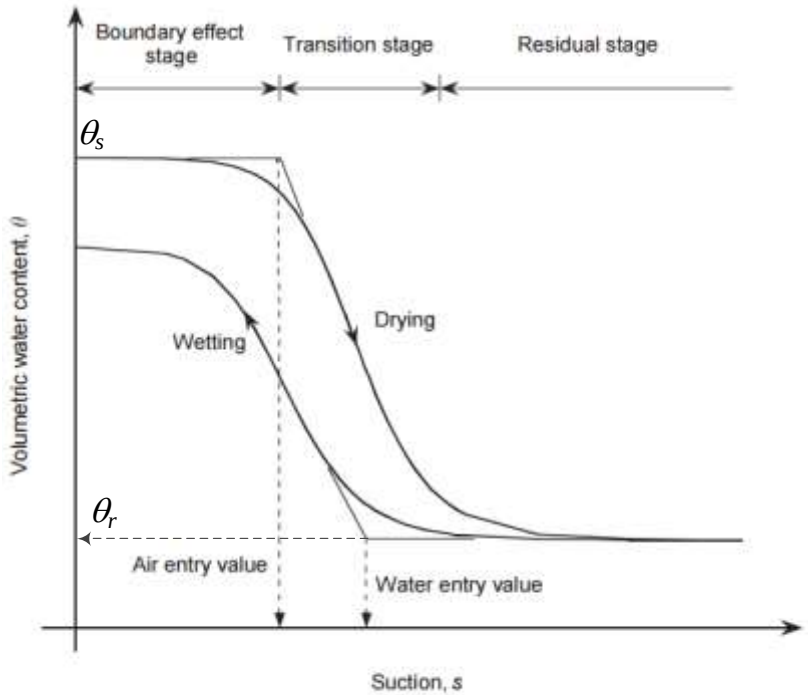

Figure 2.1: Schematic of water characteristic curve (Iryo & Rowe, 2003)

The three parameters of importance from the Water Retention curves (WRC) developed either following the wetting or drying path are the saturated water content (θ_s), which indicates the point on the WRC where all the soil pores are filled with water, the air-entry value (AEV), which indicates the suction point on the desorption curve where air first starts to enter the materials, and the residual water content θ_r, which indicates the point of water content where it becomes extremely hard to remove water from the soil (Lu & Likos, 2004).

Lu et al., (2006); Zornberg et al., (2010) report that, the WRC of geomaterial shows different wetting and drying paths, a phenomenon referred to as hysteresis. This is attributed to, during drying process, the largest pore drain first, followed by the smaller pores. In contrast, during wetting process, the small pores fill first; however, the presence of large pores may prevent some of small pores from filling. Moreover,

wetting of a dry geomaterial can lead to entrapment of air in the lager pore, preventing all the voids from filling with water.

Iryo & Rowe, (2003) conducted a study in which they reported that the overall slope of the WRC is controlled primarily by the pore-size distribution of the material. Coarse materials (sand, geotextile) with a relatively narrow pore-size distribution are marked by relatively steeper characteristic curve because the majority of pores are drained over a relatively narrow range of suction. Soils with a relatively wider pore-size distribution are marked by relatively less steep characteristic curves because the majority of pores are drained over a relatively wider range of suction. For this reason, the WRCs of clayey and silty soils have higher air-entry value compared to the WRC's sand and geotextile. Iryo & Rowe, (2003) further compared the WRC for soils and nonwoven geotextiles. They concluded that nonwoven geotextiles show steeper water retention curves and smaller air and water entry values (from 0.4 to 1.2 kPa and from 0 to 0.8 kPa for air entry and water entry values, respectively) compared to that of soils.

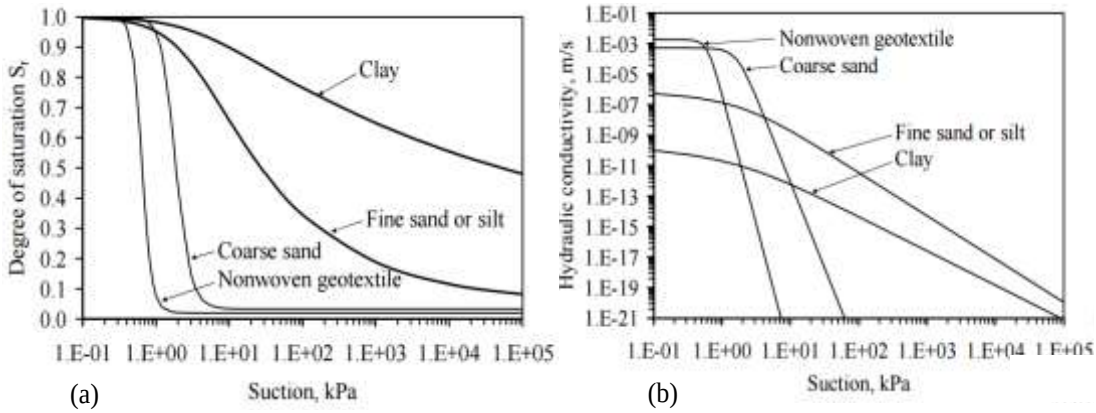

Figure 2.2: Typical hydraulic characteristic curves (Mccartney, 2007): (a) water retention curves; (b) hydraulic conductivity curves

Researchers have reported on the construction of water retention curves. Fredlund, (2006) summarized a number of common empirical equations used to best-fit soil water retention curve data, such as one by Brook and Corey of 1964, van Genuchten (1980) and one by Fredlund and Xing of 1994. Each of the proposed empirical equations for the soil water characteristic curve (SWCC) can provide the best fit to either the dry or wetting curves. Each of the proposed equations has one variable that bears a relationship to the air entry value of the soil and the second variable that is related to the rate at which the soil de-saturates. The third variable, when used, allows the low suction range near the air entry value to have a shape that is independent of the high suction range near residual conditions (Fredlund, 2006).

The most common water retention models provided in the SEEP/W databases is the van Genuchten (1980) and the Fredlund-Xing of 1994 closed form analytical expression. The closed form equation consists of four independent parameters which have to be estimated from observed soil water retention data. These types of relationships are empirical in nature with a physical basis. The van Genuchten (1980) equation is as in Equation 2.3:

$$\theta = \theta_r + (\theta_s - \theta_r) \times [1 + (\alpha \times \psi)^n]^{-(1-\frac{1}{n})} \quad \textbf{(2.3)}$$

Where;

θ_r = the residual moisture content; θ_s = the saturated moisture content; α and n = fitting parameters; ψ = matric suction (kPa)

The Fredlund-Xing of 1994 water retention model was developed based on particle size distribution of the soil. This model is similar to the van Genuchten (1980) model and is determined as:

$$\theta = \theta_r + (\theta_s - \theta_r) \times \left\{ ln \left[e + \left(\frac{\psi}{a} \right)^n \right] \right\}^m \quad \textbf{(2.4)}$$

Where;

e = base of the natural logarithm, a = represents the air entry suction, n = represents the pore size distribution, and m = represents the model skew.

SEEP/W employs the use of both the van Genuchten (1980) and the Fredlund and Xing model in the construction of the hydraulic conductivity curves.

2.3.2 Stability analysis in SLOPE/W

After infiltration and seepage analysis in SEEP/W the results are imported to SLOPE/W for stability analysis modelling. Stability analysis in SLOPE/W is carried out considering the effective stress and shear strength of the soils. The shear strength of the soils highly depend on the pore-water pressure of the soils thus the requirement of pore-water pressure results from the SEEP/W simulations.

Effective stress of unsaturated soils

In unsaturated soil engineering problems the effective stress is an important aspect in stability analysis. Bishop (1959), proposed the effective stress equation for unsaturated soil based on modifying the Terzaghi's (1942) equation ($\sigma' = \sigma - u_w$) as expressed:

$$\sigma' = (\sigma - u_a) + \chi(u_a - u_w) \quad \textbf{(2.5)}$$

Where;

σ' = effective stress; χ = coefficient of effective stress and is related to degree of saturation, and ranging from 0 to 1, 0 for completely dry soils and 1 for fully saturated ones; (σ - u_a) = net normal stress;(u_a-u_w)= soil suction .Bishop's equation relates net normal stress to matric suction through the incorporation of a soil property, χ.

However, Morgenstern, (1979) reported the limitations of Bishop's effective stress equation. First, the parameter χ when determined for volume change behaviour was found to differ when determined for shear strength. Secondly, unlike original thought, experiments were conducted in which χ was found to go beyond the boundary [0-1].

Lu & Likos, (2006), in their work investigated stresses in unsaturated soils they proposed an effective stress equation as an extension of Bishop's and an expansion of Terzaghi's equation by modifying the saturation contribution to effective stress as in Equation 2.6:

$$\sigma' = (\sigma - u_a) - [-S_e(u_a - u_w)] = (\sigma - u_a) - \sigma^s \quad \textbf{(2.6)}$$

Where;

S_e = normalized degree of saturation; σ^s = suction stress; σ - u_a = net normal stress; u_a-u_w = soil suction.

Lu, Godt, & Wu, (2010), used the van Genuchten (1980) SWCC model to determine the normalized degree of saturation as in Equation 2.7:

$$S_e = \frac{S - S_r}{1 - S_r} = \left\{\frac{1}{1 + [\alpha(u_a - u_w)]^n}\right\}^{1-1/n} \quad \textbf{(2.7)}$$

Where;

u_w= pore-water pressure; n and α = empirical fitting parameters of soil properties; S_e = normalized degree of saturation, S_r = residual saturation.

The closed form expression for suction stress for the full range of matric suction is as in Equations 2.8 and 2.9:

$$\sigma^s = -(u_a - u_w) \qquad for\ (u_a - u_w \leq 0) \qquad \textbf{(2.8)}$$

$$\sigma^s = -\frac{\left((u_a - u_w)\right)}{\left\{\frac{1}{1 + [\alpha(u_a - u_w)]^n}\right\}^{\frac{(n-1)}{n}}} \qquad for\ (u_a - u_w \geq 0) \qquad \textbf{(2.9)}$$

Lu et al., (2010) proposed a closed form equation for effective stress in the entire pore-water pressure range (all saturations levels) the closed forms equations are illustrate as Equations 2.10 and 2.11:

$$\sigma' = \sigma - u_a + (u_a - u_w) \qquad for\ (u_a - u_w \leq 0) \qquad \textbf{(2.10)}$$

$$\sigma' = \sigma - u_a + \frac{\left((u_a - u_w)\right)}{\left\{\frac{1}{1 + [\alpha(u_a - u_w)]^n}\right\}^{\frac{(n-1)}{n}}} \qquad for\ (u_a - u_w \geq 0) \qquad \textbf{(2.11)}$$

The closed form equation require only two controlling parameters: the inverse of air entry pressure, α, and pore size spectrum number, n. Therefore, the proposed closed form equation for effective stress can be considered to be a unified description for phenomena of flow and stress on porous granular materials. With the proposed equation the transition from saturated to unsaturated states is continuous and smooth,

ensuring mathematical consistency between Terzaghi's (1942) equation and the proposed equation.

Using the proposed effective stress equation has the important practical implication since there is no need for any new shear strength criterion for unsaturated soil and the need for the determination of the coefficient of effective stress χ as in Bishop's (1959) formulation.

Unsaturated soil shear strength

Initially, the shear strength of the unsaturated soil was defined in terms of a linear increase with matric suction. The linear increase in shear strength was designated using an angle ϕ^b, which has the character of friction angle. This assumption was found to overestimate the shear strength when the matric suction is high. Lu et al., (2006), reported that depending on the type of soil and the prevailing matric suction, the effective stress can either increase or decrease as matric suction increase. A number of researchers (Villar,2006; Khalili et al,1998; Bao et al,1998;Fredlund et al,1996; Vanapalli et al, 1996) as cited in Zhang et al., (2014) reported that the use of nonlinear shear strength for the unsaturated shear strength for unsaturated soil can provide a more realistic simulation of field conditions. Figure 2.3 shows the illustration of the general anticipated unsaturated shear strength envelopes for 3 typical soils.

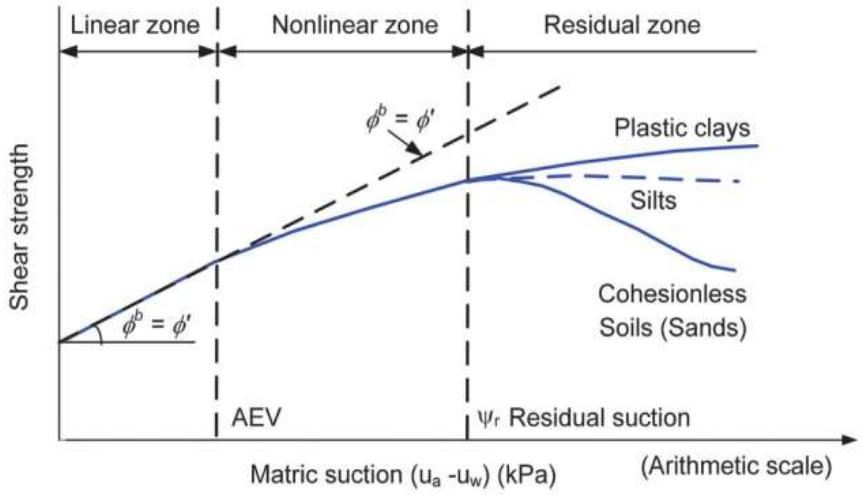

Figure 2.3: The relationship between unsaturated shear strength envelope and matric suction (Zhang et al., 2014)

As a better alternative to the use of ϕ^b, SLOPE/W implemented the Equation 2.12 proposed by Vanapalli et al., (1996) to quantify the unsaturated soil shear strength:

$$\tau_f = c' + (\sigma_n - u_a)\, tan\, \phi' + \frac{\theta_w - \theta_r}{\theta_s - \theta_r}(u_a - u_w) tan\phi \qquad \textbf{(2.12)}$$

Where

τ_f = shear strength; c' = effective cohesion intercept for a saturated soil; σ_n–u_a = net normal stress on the failure plane; σ_n = total normal stress; u_a = pore air pressure; ϕ' = effective friction angle; u_a–u_w = matric suction; u_w = pore-water pressure; θ_w = volumetric water content; θ_s = saturated volumetric water content and θ_r = residual volumetric water content.

According to Equation 2.12, the shear strength contributed by soil suction becomes zero when the soil suction is greater than the residual suction. The shear strength equation shows a nonlinear relationship from the saturated to residual soil condition.

Stability analysis

According to FHWA (2009) design guideline the lateral earth pressure method has been recommended for designing reinforced wall while the limit equilibrium has been used for designing the reinforced slopes. The slope and wall distinguish by the face inclination β (slope $\beta<70^{o}$, wall $>70^{o}$). The limit equilibrium method (LEM) assumes a potential slip surface, the soil along the slip surface providing the shear resistance, and geosynthetic reinforcement providing tensile force and resistance moments. The stabilizing forces contributed by the reinforcement layer are incorporated into the equilibrium equations to determine the factor of safety of the reinforced mass. The slope is divided into a number of vertical slices then the equilibrium equations (equilibrium of the forces and/or moments) are written and solved for each slice.

There are several limit equilibrium methods that have been developed to help analyse the stability in slopes. The ordinary or Swedish method for circular slip surfaces being the first, the method is simple and best suited for hand calculations. Bishop in 1955 advanced the method introducing a new relationship for the base forces of the slices, this was necessitated by the fact that the ordinary method resulted in linear factors of safety which in the real application is not realistic. The Bishop method thus advanced and improved to give a much better realistic non-linear factors of safety. Improvement on the analysis method resulted in the Morgenstern-Price (1965), Spencer (1967), methods which satisfied both moment and force equilibrium conditions in the analysis of the vertical slices stability. Generally, all the limit equilibrium based methods are based on the assumptions for the vertical slice normal and shear forces. In addition to this, the shape of the assumed slip surfaces and the equilibrium conditions for the calculation of the factors of safety.

The limit equilibrium method has been found adequate in the analysis of the safety of embankments and slopes. It compared well to the Finite element analysis of stability. Maula et al., (2011) in a study that aimed at investigating the effects of earthquake on the stability of slopes used two commercially available software Plaxis 2D program (FEM based) and Geo studio's SLOPE/W 2007 (LEM based). They compared the results obtained from the two numerical experiments. From the study they reported that the results of the two numerical experiments resulted in expected results from normal computations, they reported that the factor of safety reported from the FEM were a bit higher as compared to those of LEM analysis.

Similar results on the performance of LEM based analysis were reported by Ashraf et al., (2012). In the study they reported that analysis of factor of safety and strength reduction factor computed by both LEM and FEM indicated a difference of values which were less than 6%. This was based on an investigation into the factors of safety of slopes when exposed to various causes of instability. This study employed the use of LEM based software SLOPE/W. The pore-water pressures firstly will be predicted in FEM based SEEP/W, and then imported to LEM based SLOPE/W to determine the factor of safety. Table 2.2 presents the descriptions of LE methods available in GeoStudio.

The factor of safety in Geo-Slope (2007) was defined by assuming that, the reinforcement in the embankments increases the shear resistance as shown in equation 2.13. The implication is that the soil shear resistance and reinforcement shear resistance are developed and mobilized at the same rate.

$$FoS = \frac{Soil\ Shear\ strength + reinforcement\ resistance}{shear\ stress\ required\ for\ equilibrium} \quad \textbf{(2.13)}$$

Table 2.2: Descriptions of equilibrium methods of slope stability analysis

Method	Overall Moment Equilibrium	Individual Slice Moment Equilibrium	Horizontal Force Equilibrium	Vertical Force Equilibrium	Assumptions	Comments
Ordinary of Fellenius (1927)	Yes	No	No	No	Circular slip surface Side Force Parallel to Base	Conservative and very inaccurate for high water pressures
Bishop's Modified (1955)	Yes	No	No	Yes	Circular slip surface Side Forces Horizontal	Very inaccurate for high water pressures
Morgenstem and Price (1965)	Yes	Yes	Yes	Yes	Slip surface of any shape Pattern of side Force Orientations	Much engineering time required to vary side force assumptions
Spencer (1967)	Yes	Yes	Yes	Yes	Slip surface of any shape Side force parallel	Accurate method
Corps of Engineering (1970)	No	No	Yes	Yes	Slip surface of any shape Side force parallel to slope	High factor of safety
Lowe and Karafiath (1960)	No	No	Yes	Yes	Slip surface of any shape Side force orientation average of slope and slip surface	Best side force assumptions
Janbu Simplified (1954)	No	No	Yes	Yes	Slip surface of any shape Side force horizontal	Low factor of safety
GLE (Fredlund et al. 1981)	Yes	Yes	Yes	Yes	Slip surface of any shape Pattern of side force orientation	Much engineering time required to vary side force assumptions

2.4 Performance of Geotextile in Reinforced Embankments

Despite the advantages of drainage and stability that geotextile layers provide studies have reported that capillary barrier develops when an unsaturated fine-grained soil layer is underlain by another unsaturated porous material with relatively large-sized pores, such as a coarse-grained soil layer (e.g. sand or gravel), or a porous geosynthetic e.g. a nonwoven geotextile (Zornberg et al., 2010). The main impact of the capillary barrier effect is that a measurable amount of water will not flow from the fine-grained soil into the underlying coarse material until a critical condition is reached (Zornberg et al., 2010) . Because of this, the capillary break effect has been observed to increase the water storage capacity of soils beyond the level that would normally drain under gravity (Khire, Benson, & Bosscher, 2000).

Main factors that influence the capillary barrier effect phenomena are the hydraulic characteristics of materials under unsaturated conditions. Near saturation, the coarser materials have the higher hydraulic conductivity than that of the fine grained materials (Yang et al., 2017). However, as the water content decreases the hydraulic conductivity of sand or nonwoven geotextiles decreases faster than that of fine-grained soils. Hence, the hydraulic conductivity of nonwoven geotextile is lower than that of fine materials under unsaturated conditions, and nonwoven geotextile works as hydraulic barrier. Since the fined grained material can retain more water in the pores as suction increases they have more pathways available for water flow and are thus more conductive than coarser materials.

García-aristizábal et al., (2016) in the study on the infiltration in unsaturated soil-geosynthetics reported that geosynthetics embedded in slopes backfill behave like an

impermeable layer when embedded in unsaturated surrounding soils. Similar studies were conducted by Garcia et al., (2007) and reported that measurable amount of water did not flow from fine grained soil to nonwoven geotextile until the soil was nearly saturated due to capillary barrier effect. Increase in the water content at the soil-reinforcement interface can trigger local slope failure of the soils immediately above the geosynthetic layer during infiltration.

On the performance of the non-woven geotextile when inclined; Iryo et al., (2005) reported on the effect of inclining the non-woven geotextile at a 10% on the drainage of the embankment. They reported inclining the geotextile material reduces the amount of water that accumulates in the upper zone of the geotextile material. The water will drain due to the slope created as a result of inclining the geomaterial. They reported that inclining the geotextile at 10% inclination made it more effective in its performance as a draining medium. Figure 2.4 illustrates the inclination reported by Iryo and Rowe. Similar results were obtained by Miyazaki (1988) as cited in Iryo et al., (2005) who reported that water did not actually drain from the geotextile layer but, rather from the interface above the soil layer. This helps to reduce the amount of water that accumulates above the non-woven geotextile due to capillary barrier.

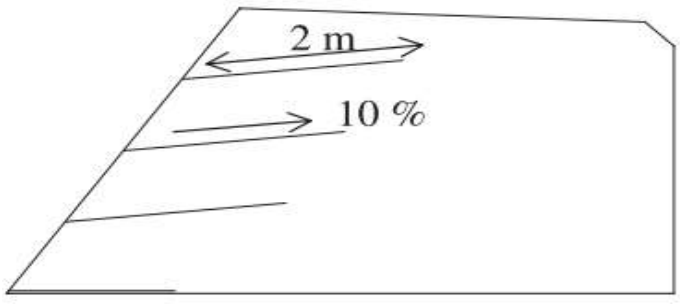

Figure 2.4: Geotextile inclination in unsaturated soils backfill (Iryo & Rowe, 2005)

It is observed that non-woven geotextile can work effectively as drainage materials in conditions where the pore-water pressures are positive (saturated conditions). On the contrary, in conditions where the pore-water pressures are negative (unsaturated conditions), nonwoven geotextile have been reported to work as a moisture barrier rather than as drainage. Not much work has been reported on the effect of inclining the non-woven geotextile layer however the few have reported an improvement on the overall drainage.

2.5 Sand Cushions on the Performance of Marginal Soils Backfill

Marginal soils have been reported to possess medium to high plasticity. The cohesive property of the marginal soils comes into play in the behaviour of reinforced marginal soils. The interface efficiency C_i which is the ratio of interface strength between the soil and reinforcement to shear strength of the soil and is an important design parameter for reinforced soils. Interface efficiency is used to calculate the effective length of the reinforcement required beyond the critical failure plane for MSE walls and reinforced slopes. Interface efficiencies for cohesive soils and non-cohesive soils are determined by Equation 2.14 and Equation 2.15, respectively

$$C_i = \frac{c_a + \sigma_n tan\delta_a}{c + \sigma_n tan\emptyset} \quad \textbf{(2.14)}$$

$$C_i = \frac{tan\delta_a}{tan\emptyset} \quad \textbf{(2.15)}$$

Where;

c_a = interfacial cohesion; δ_a = interfacial friction angle; ϕ = soil friction angle; c = soil cohesion; C_i = interface efficiency; σ_n = normal stress.

According to Equation 2.14 and Equation 2.15, C_i is only a function of the characteristics of soil and geosynthetics for non-cohesive soil, while for cohesive soil, C_i also depends on the normal stress. Therefore, the reinforcement efficiency depends on multifactor including soil type, normal stress and type of geosynthetics. An interaction coefficient greater than unity ($C_i > 1$) indicates that there is an efficient bond between the soil and the geosynthetic and the interface strength between the soil and the reinforcement is greater than the internal shear strength of the soil. Similarly, if the interaction coefficient is less than 0.5 ($C_i < 0.5$) indicates weak bonding between soil and geosynthetic or breakage of geosynthetic layer. A number of studies on interface efficiency have been conducted.

Murad et al., (2007) conducted studies on cohesive soil-geosynthetics interactions based on laboratory testing. The study involved three clay samples of different plasticity and a sand sample. The soils were reinforced with geosynthetics material and the soil-geosynthetic interface parameters obtained. They reported that geogrids can successfully be used as reinforcements in cohesive soils the resulting interface efficiency C_i was reported to be greater than 0.7 showing a good bond exists between clayey soils and geogrid. However they further concluded that levels of normal stresses soil type and geosynthetic type have a great contribution in determining the interface efficiency.

Choudhary et al., (2016) studied three types of cohesionless soils reinforced with different types of geosynthetics materials. Pull-out tests by use of large direct shear test were conducted to investigate the interface behaviour of soil-geosynthetics. Geosynthetics that allowed the penetration of soil particles within themselves such as

the non-woven geotextile were found to possess higher soil-geosynthetic inter- face friction angle values than those of woven geotextile. Pull-out interaction coefficients C_i were reported in the range 0.62-1.72.

From the above literature non-woven geotextile can be used to increase both the drainage and stability property of the marginal soil embankment. Cohesive soil have been found to have an adequate pull-out resistance when a non–woven geotextile is used although lower than that of non-cohesive soils. Sand layers provision to sandwich the non-woven geotextile have been suggested to improve on the inter-face friction angle and subsequent improvement of the pull-out resistance of the geotextile material. A number of studies have been conducted and reported on the improvement of the pull-out resistance of the non-woven geotextile in such arrangements.

Lin et al., (2014) conducted an experimental research to investigate the efficiency of sandwiching the geotextile material in thin sand layers. They observed that presence of the sand layers greatly improved on the drainage. They also reported the sand cushion improved drainage by reducing the water ingression and long-term clogging in the nonwoven geotextiles by fine-grained soil. Addition of the number of the sand cushion had an improvement in the overall drainage of the slopes.

Raisinghani et al., (2010) conducted an experimental research to examine the permeability of confined marginal soils with embedded geosynthetics layers. In the research a permeameter was custom designed and the permeability tests carried out on the varying marginal soils. With increase in normal stress it was observed that there was a subsequent decrease in the permeability characteristics of geosynthetic-reinforced soils however, by sandwiching the geosynthetics layers with thin sand

layers cushions they reported an improvement in the equivalent coefficient of permeability by upto 180 times as compared to without the sand cushions. Sand cushions in this research were also observed to have contributed in the levels of clogging of the geosynthetic material in the set-up.

Abdi et al., (2014) in their experimental research investigated ways of enhancing the pull-out resistance of GRS structure composed of clay and geogrid. They investigated three setups a sand-geogrid, clay-geogrid and clay sand–geogrid. In the study they reported provision of a thin sand layer around the geogrid greatly enhanced the pull-out resistance and improved the strength and deformation characteristics of reinforced clay by improving the soil-reinforcement interface shear strength.

From the above studies sand cushion layers have majorly been provided to aid improve the drainage and pull-out resistance of the non-woven geotextile material. The effect on the thickness of the sand layer on the overall stability of the embankment has however not been investigated. This study will look into the effect of sand layer provision on the drainage and stability of the embankment.

2.6 Research Gap

From the literature, failure of GRS structures has been attributed to a number of factors that include external loading, poor drainage and choice of materials. A number of studies carried external loadings on GRS structures and self-weight of the geomaterial in the backfill. Marginal soil have been used as backfill materials although a number of failure cases largely attributed to poor drainage have been reported. Notably, most of the researches did not consider the aspect of extreme rainfall in the design of GRS

structures, which has largely been attributed to failure of most GRS structures made of marginal soils. Studies by Thuo et al, (2015); Lin et al, (2014) have reported an improvement on the pull-out resistance of GR marginal soils embankments with thin sand cushions. However, from the previous studies the effect of providing sand cushion layers on the improvement of the stability of embankments have not been comprehensively studied, optimum sand cushion thickness for use within reinforced locally available backfill soils have not been reported and research on the optimum spacing of drainage layers for use within reinforced walls with locally available soils as backfill have not been studied. In light of this, this study aims at addressing this gap by investigating the optimum angle for geotextile inclination, the contribution of sand layer thickness on the performance of red coffee soils embankments and the determination of appropriate drainage layer intervals. This will be conducted by evaluating the optimum placement of sand cushions in GRS embankments subject to rainfall infiltration. This study is meant to compliment previous studies on the drainage of GRS embankments. Results of the study will aid in developing improved methodologies in the design and construction of embankments from marginal soils.

2.7 Conceptual framework

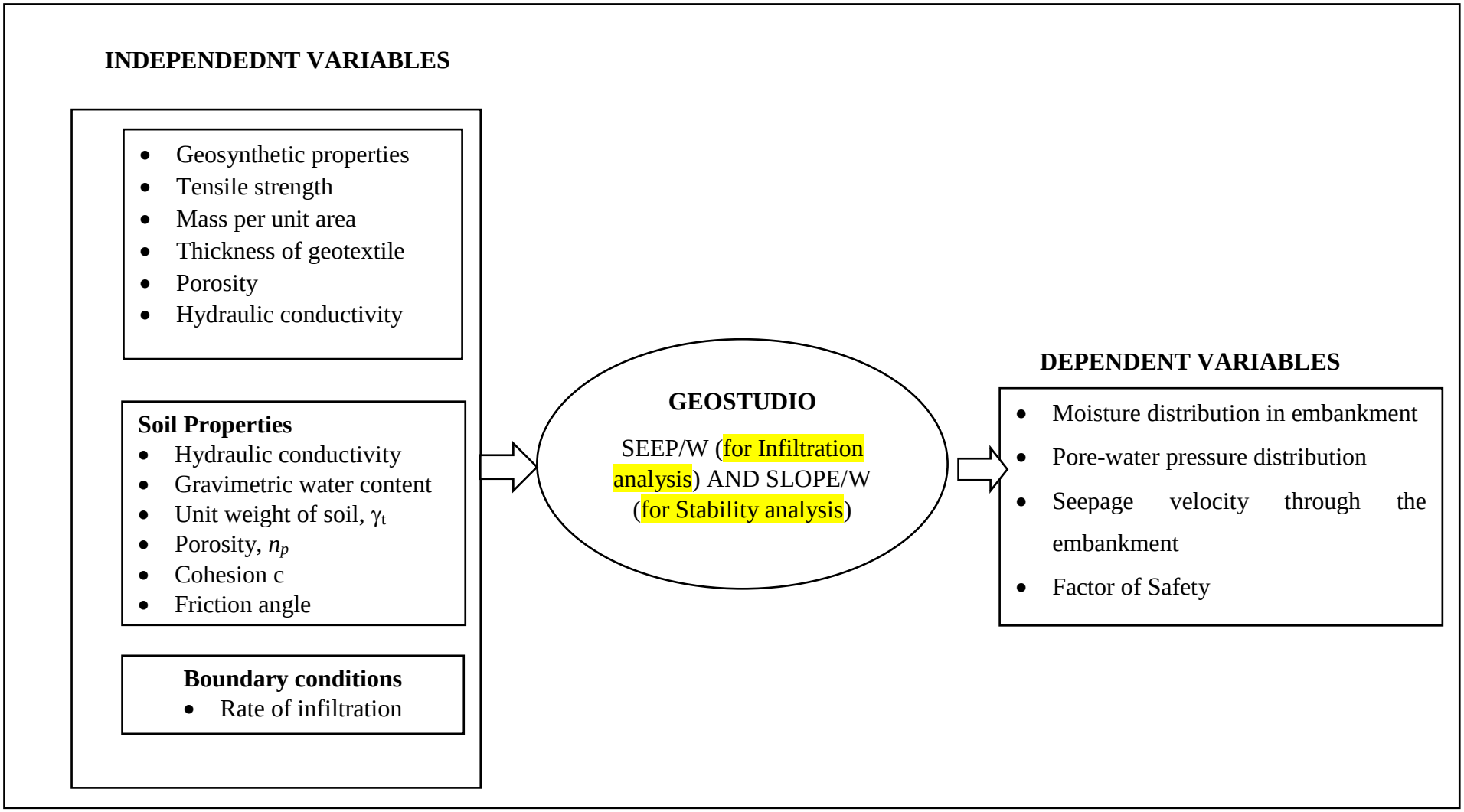

CHAPTER THREE

MATERIALS AND METHODOLOGY

3.1 Introduction

This chapter covers the overall methodology that was adopted in meeting the objectives of the research. The chapter introduces the overall research design covering model validation, material laboratory tests, and numerical studies.

3.2 Overview of the Tests and Procedures

The research design adopted for this research was a combination of laboratory tests and numerical model simulations. Laboratory tests were carried out to give the parameters of the RCS and the river sand to be used in the numerical modelling. A numerical model based on Iryo and Rowe reporting of the PWRI works was first developed and validated for its accuracy using SEEP/W in modelling infiltration into unsaturated soils. After the suitability of the model was confirmed, the geosynthetic reinforced soils slopes with rainfall were then simulated to achieve the objectives of the study. Rainfall data to be used in the research was obtained from the meteorological department of Kenya while the red coffee soils was obtained from Juja, Kiambu County in Kenya. Laboratory tests was carried out in the JKUAT/PAUISTI Civil Engineering Laboratories.

3.3 Materials

3.3.1 Red coffee soils

RCS are readily available in most regions of the central part of Kenya. The granular RCS for this study was sourced from Juja area, Kiambu County. The soil was collected at a depth of 1.5m from the ground surface. This was to minimise collection of organic matter such as roots which affect properties during testing of the soil. Soil at this depth

has little amounts of contamination with other soils that could have been transported to the area.

3.3.2 Sand

In this study river sand formed part of the drainage layer and were used to sandwich the geosynthetic material. The river sand used in the study was sourced from local dealers in Juja Town.

3.3.3 Rainfall data

Rainfall data for the study was obtained from the Meteorological Department of Kenya for the Dagoretti station between the periods January 1990 to December 2017. The Dagoretti station is located in Nairobi County of Kenya.

3.3.4 Numerical Program

The numerical programs from GeoStudio 2012 were used in the analysis in this study. Finite element program SEEP/W was used in the seepage analysis while Limit Equilibrium software SLOPE/W program from GeoStudio was used for the stability analysis.

3.4 Methodology

3.4.1 Modelling infiltration in unsaturated soils backfill using SEEP/W

3.4.1.1 Model calibration

In order to calibrate the numerical model SEEP/W in the simulation of infiltration into unsaturated backfill embankments, experimental results performed by the public works research institute of Japan as reported by Iryo et al., (2005) were used. For the experiment, a series of numerical model simulations with different mesh configurations, boundary conditions, time steps and different approaches to achieve

initial conditions were used to establish a suitable numerical scheme. In order to achieve the model calibration, results predicted using numerical analyses were compared with those obtained through experimental observations.in the comparison the coefficient of determination was evaluated and the suitability of the SEEP/W model in predicting infiltration established. Where necessary, approach, time steps or the boundary conditions were adjusted accordingly in order to suite predicted results to measured ones.

Experimental setup

In investigating infiltration into unsaturated soil backfills, Iryo et al., (2005) reported on performance of full scale embankments tests performed by Public Works Research Institute of Japan (PWRI). The study investigated the effect of artificial rainfall on the performance of unreinforced embankment which was labelled as Embankment 1. Sandy soil with material properties as shown in Table 3.1 was used as backfill material.

Table 3.1: Properties of the backfill sandy soil

Gravel content ($d \geq 2$ mm), (%)	1
Sand content ($2 > d \geq 0.074$ mm), (%)	91
Fine Content ($d < 0.074$ mm), (%)	8
Gravimetric water content, ω (%)	24
Unit weight of soil, γ_t (kN/m^3)	17.5
Porosity, n_p	0.465
Saturated hydraulic conductivity, k_{sat} (m/s)	1.3 x 10^{-5}
Friction angle, ϕ' ($^\circ$)	39
Cohesion c' (kPa)	0

The embankment was 3 m high, 6 m long, and 4 m wide with a sloping side of 1V: 0.7H as shown in Figure 3.1. A 4% gradient towards the back of the embankment was

maintained at the top face of the embankment. The embankment was set on an impermeable concrete base. The back fill soils were placed at 24 % gravimetric water content compacted in layers of 150 mm using a hand held vibratory roller to achieve an average uniform density of 17.5 kN/m^3. To avoid development of pore-water pressures at the base, a 1.5 m long geotextile layer was placed at the bottom of the embankment

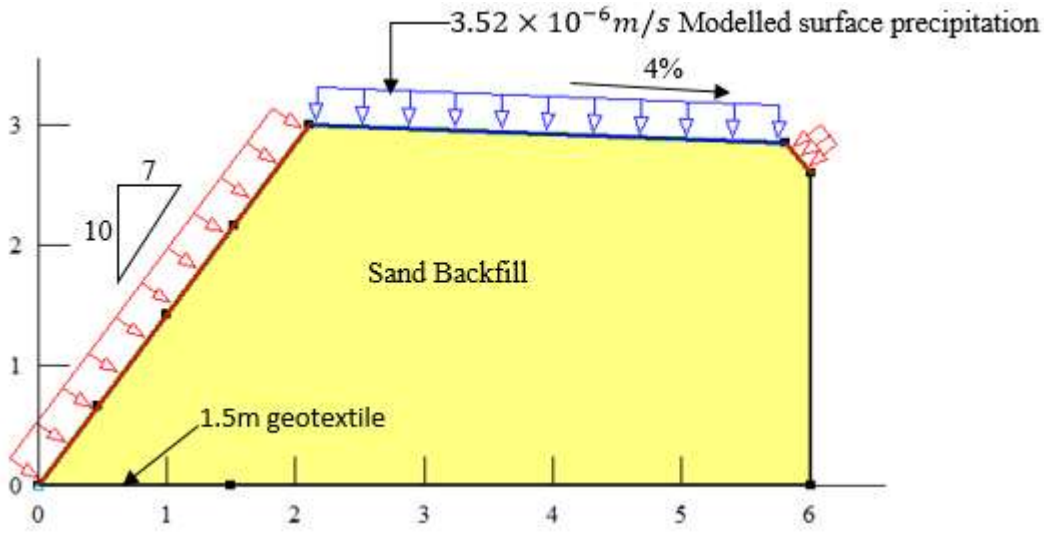

Figure 3.1: Experiment setup model of unreinforced embankment subjected to rainfall infiltration (Iryo & Rowe, 2005)

After the embankment was constructed, artificial rainfall with an intensity of 12.7 mm/h (q= 0.24 $k_{sat\ soil}$) was applied as $3.52 \times 10^{-6} m/s$ and $2.02 \times 10^{-6} m/s$ corresponding to the flat top surface and sloping surface. During the experiment, water content within the embankment was monitored using the radio isotope method along three vertical observation lines (x=1.2 m, 2.4 m, and 4.8 m from the toe).

Numerical simulation

To simulate the experimental setup conducted by the PWRI, transient seepage analysis was carried out to calibrate the finite element program SEEP/W. The Richards

equation for water flow within unsaturated material as shown in Equation 2.1 was applied in SEEP/W. The van Genuchten (1980) model was employed in the determination of the hydraulic properties function and the water characteristic curve of the backfill sand and the non-woven geotextile.

In the study the embankment was modelled using a series of numerical experiments with different mesh configurations and time steps. The mesh configurations were composed of the quad and triangles mesh combination and the purely triangular mesh. The illustration of the mesh configuration is as shown in Figure 3.2.

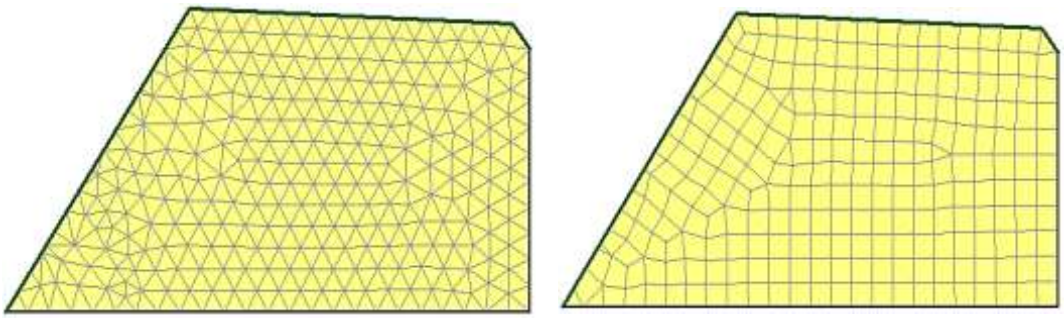

Figure 3.2: (a) Triangular mesh configuration and (b) the quad &triangles mesh configuration

The height of the finite elements was adjusted from 0.25m to 0.05m with the time steps automatically being adjusted between 0.1 second and 100 seconds. The rainfall intensity of 12.7mm/h was applied as unit flux (q) on the flat side as and sloping side of the embankment. To establish initial pore-water condition before simulation of rainfall infiltration, a steady-state seepage analysis with prescribing a unit flux on prescribed unit flux on the surface boundaries was done. The values of prescribed unit flux were adjusted until when matrix suction did not exceed initial soil conditions.The non-woven geotextile at the bottom of the embankment was modelled as a line with 3 mm interface elements. The volumetric water content data in the simulated model was

measured at a distance x=1.2, 2.4 and 4.8, in both triangular and quadrilateral shaped finite elements models at elevations similar to those of the experimental setup.

3.4.1.2 Model validation

Upon the calibration of the numerical model SEEP/W the numerical model validation was conducted. This was done using experimental results of two other reinforced embankments done by the Public Works Research Institute (PWRI) of Japan labelled as embankment 2 and 3. The embankments labelled embankment 2 and 3 are as shown in Figure 3.3.

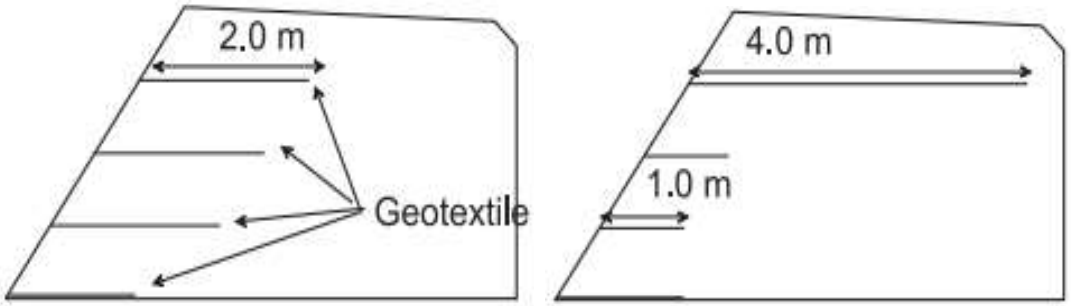

Figure 3.3: Outline of the modelled embankments (a) Embankment 2 (b) Embankment 3

In evaluating the performance of reinforced embankments subjected to infiltration, Iryo et al., (2005) reported the experimental setup done by the PWRI on the reinforced embankments labelled embankment 2 and embankment 3. The two embankments were of height 3m with a cross-sectional length of 6m. The sloping side of the embankment was inclined at an angle of 55°. In the set up embankment 2 was reinforced with four layers of 2m long geotextile layers spaced at an interval of 0.75m with a layer of geotextile placed at the bottom of the embankment to aid in the draining of the embankment. Embankment 3 was composed of four layers of non-woven geotextile

spaced at 0.75m. Ten centimeters of the non-woven geotextile layers protruded out of the sloping side of the embankment. Properties of the non-woven geotextile used in the experiment are as presented in Table 3.2

Table 3.2: Properties of non-woven geotextile used in the experimental setup

Mass per unit area, m_a (g/m^2)	310
Thickness of geotextile, $t_{geotextile}$ (mm)	3
Porosity, n_p	0.92
Saturated hydraulic conductivity in plan direction, $k_{sat\ geotextile\ plane}$ (m/s)	$2.3x10^{-2}$
Saturated hydraulic conductivity in cross plane direction, $k_{sat\ geotextile\ cross}$ (m/s)	$3.5x10^{-3}$
Tensile strength in machine direction (kN/m)	21.6
Tensile strength in cross to machine direction (kN/m)	17.2

Similar to embankment 1 used in the calibration of the SEEP/W model the soil back fill (with properties as shown in Table 3.1) were placed at 24 % gravimetric water content and compacted in layers of 190 mm using a hand held vibratory roller to achieve an average uniform density of 17.5 kN/m^3. Artificial rainfall with an intensity of 12.7 mm/h (q= 0.24 $k_{sat\ soil}$) was applied as $3.52 \times 10^{-6} m/s$ and $2.02 \times 10^{-6} m/s$ corresponding to the flat top surface and sloping surface boundary conditions respectively. During the experiment, water content within the embankment was monitored using the radio isotope method along three vertical observation lines (x=1.2 m, 2.4 m, and 4.8 m from the toe).

In the numerical validation process the embankments were simulated. Time steps and mesh configurations obtained in the calibration process were applied in these numerical models. The embankments were modelled using quad elements of 0.1m height arranged as shown in Figure 3.4. The element global height was set to 0.1m constrained to a third of global element size on top side and lower side of geotextile.

Time increment was automatically set between 1-100 seconds as required to achieve convergence. The non-woven geotextile layers as in the experimental setup protruded out of the embankment on the sloping side. Boundary conditions specified on the embankments were the artificial rainfall with an intensity of 12.7 mm/h that was applied as a unit flux of $3.52 \times 10^{-6} m/s$ for the embankment top and as a unit flux of $2.02 \times 10^{-6} m/s$ corresponding to sloping surface, a zero flux boundary condition was prescribed for the bottom part of the embankment.

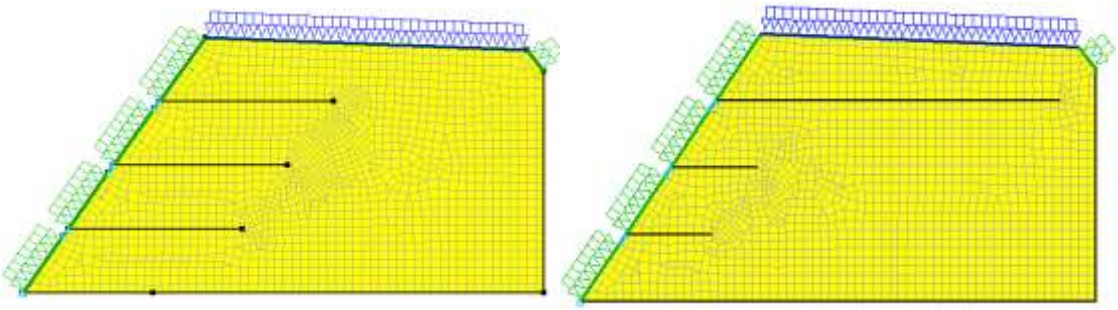

(a) (b)

Figure 3.4: Numerical model set up of the validation (a) embankment 2 (b) embankment 3

3.4.1.3 Data analysis

In the calibration of the model, data was analysed by comparing the experimental data to the predicted data obtained. The simulated output and experimental results were statistically analysed using the Root Mean Square Errors (RMSE) and coefficient of determination were determined. This was done using Ms excel 2013 functions. Acceptance of the adjustments made to the model was based on how close to 1 the R^2 value was and how low the RMSE.

$$R^2 = \left\{ \frac{1}{n-1} * \frac{\sum(x - \bar{x}) * (y - \bar{y})}{(\sigma_x * \sigma_y)} \right\} \quad \textbf{(3.1)}$$

Where: x refers to the experimental values, $\bar{x}$ the mean of the experimental results, σ_x standard deviation of the experimental results, y refers to the modelled predicted

results, $\bar{y}$ the mean of the modelled results, σ_y is the standard deviation of the modelled results and n the number of observations.

$$RMSE = \left(\frac{1}{n} * \sum_{i=1}^{n} (y_{pred} - x_{experi})^2\right)^{1/2} \quad \textbf{(3.2)}$$

Where: N refers to number of observations, y_{pred} is the model predicted results and x_{experi} is the actual experimental results

In the validation of the model predicted data was analysed using the coefficient of determination and a coefficient of determination closer to that obtained in the calibration was accepted. The coefficient of determination was obtained using Equation 3.1.

3.4.2 Effect of non-woven geotextile layers inclination on the drainage and stability of RCS embankments

In order to determine the effect of the non-woven geotextile inclination on the performance of RCS embankments. Properties of the RCS were first determined. This was based on laboratory testing of the engineering properties of the RCS. The properties of the non-woven geotextile used in the study were obtained from secondary sources to reflect the properties of non-woven geotextiles in the market. After the determination of the RCS properties numerical simulations on the RCS were conducted to evaluate the performance of the embankments when subjected to rainfall infiltration. Rainfall data was important in the specification of the boundary conditions of the embankments and was obtained from the meteorological department of Kenya.

3.4.2.1 Properties of RCS

Properties of the RCS were carried out based on the relevant American Society for Testing and Materials (ASTM) standards. When the sampled material reached the lab

the moisture content of the RCS sample was first determined. This was carried based on the ASTM D4643, (2017). Specific gravity test of the RCS was conducted in accordance with ASTM D854, (2014). Since a large portion of the RCS managed to pass through the 0.475mm sieve, the grain size distribution was determined quantitatively from sieve (ASTM D6913, 2017) and hydrometer analysis tests (ASTM D7928, 2017). Atterberg limit test (ASTM D4318, 2017) was carried out to determine liquid limit, plastic limit and plastic index of the RCS. Based on the particle size distribution and the plasticity index of the RCS. The RCS was classified according to Unified Soil Classification System (USCS) using the (ASTM D2487, 2017).

Having classified the RCS and determined the gradation of the soil the optimum moisture content and maximum dry density of the soil (ASTM D698, 2012) were determined. The standard compaction test which entails 25 blows on the soil confined in the holding cylinder was carried out. The optimum water content ensures that the compacted soil at that moisture content attains the maximum density when compacted. This reflects the conditions in which the RCS will initially exist during the construction of the embankments.

Isotropically consolidated undrained (CU) triaxial compression tests (ASTM D4767, 2011) was carried out to determine the strength parameters of the RCS with pore pressure measurements. The RCS material specimens was compacted to the field density corresponding to 90% of its maximum dry unit weight obtained from the standard compaction test. The samples were saturated to achieve a Skemptons B values of around 87%. The samples were then consolidated to confining pressures of 70, 100

and 150kPa for a period of 24 hours until the consolidation process was insignificant before the compression of the specimen was conducted to failure.

Hydraulic conductivity tests were conducted to determine the permeability property of the RCS and the river sand. Hydraulic conductivity is an important aspect in the determination of embankments stability. The constant head method was used in the determination of the hydraulic conductivity of RCS.

3.4.2.2 Numerical simulations

The numerical simulations done on the RCS embankments entailed both the seepage and stability modelling. The modelling first involved the seepage simulations. After the seepage analysis the results were imported to SLOPE/W model for slope stability simulations.

Seepage modelling procedure in SEEP/W

The seepage analysis procedure in seep/w involved first sketching the embankment problem. Appropriate sketching tools that included point, polylines were used to come up with the embankment. The model setup is as shown in Figure 3.5. After the embankment was drawn regions in which the RCS backfill would occupy in the embankment materials were defined. The non-woven geotextile material was modelled as a line with 3 mm interface elements. Six embankments were modelled based on the different angles of inclination of the non-woven geotextile layer. The different angles applied in this study were 0°, 1°, 3°, 4.5°, 6°, 7.5°, 9° and 10.5° above the horizontal.

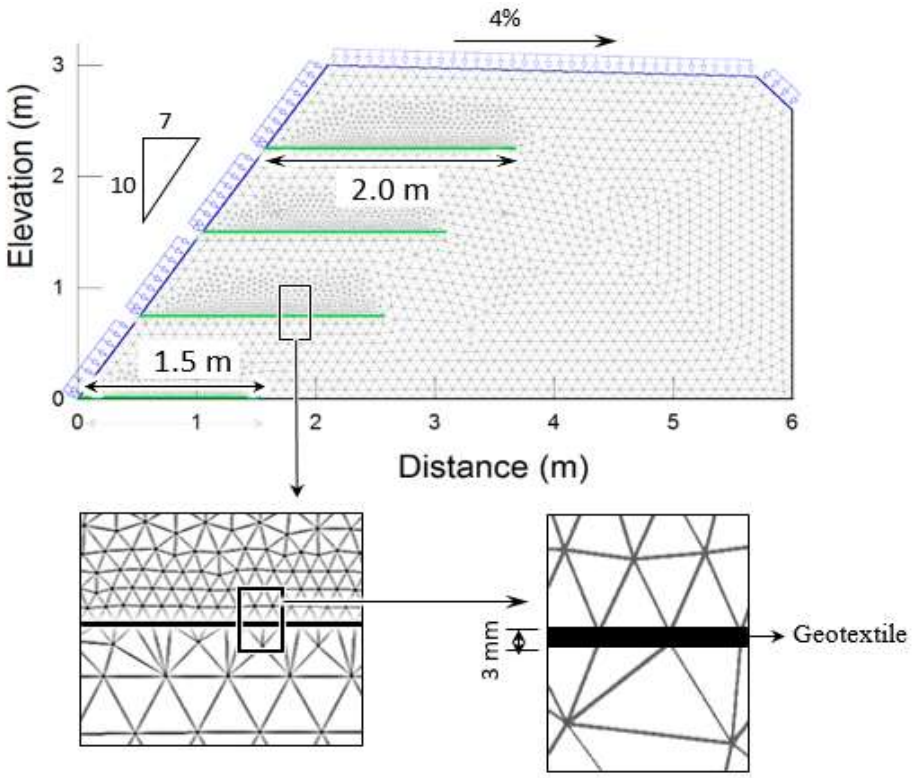

Figure 3.5: Numerical model set up to investigate inclination angle of the non-woven geotextile

The next step involved keying in the material properties. For the RCS, these were the values obtained from the laboratory test results. The materials modelled were taken to be 'isotropic' and 'saturated- unsaturated'. As shown in Figure 3.6

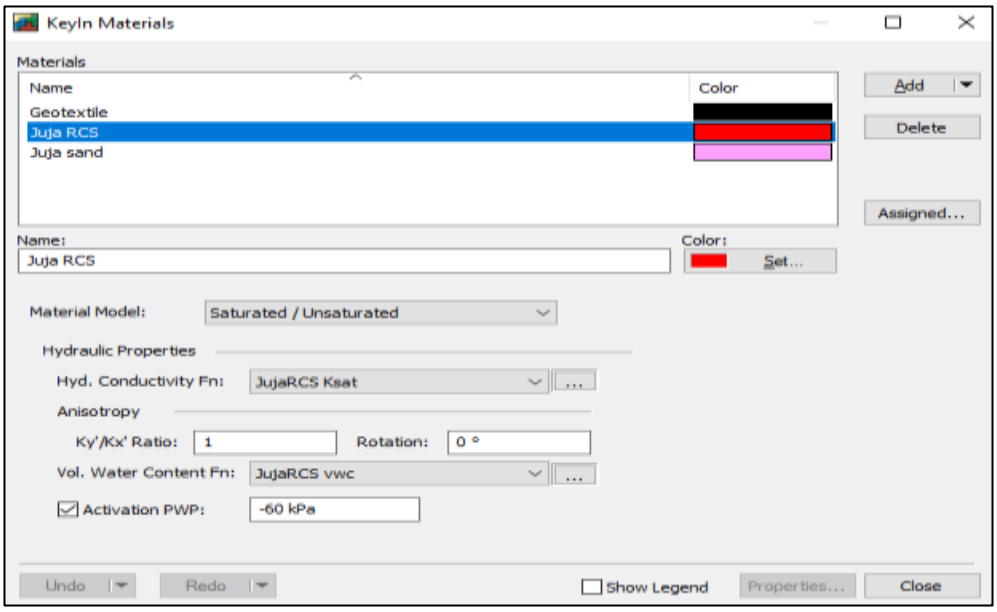

Figure 3.6: Typical SEEP/W Material key in dialogue box

In the definition of the volumetric water content functions, ‘sample functions’ were used with ‘silty clay’ used for the function of RCS. The Fredlund and Xing method was used to obtain the hydraulic conductivity function of the RCS as shown in Figure 3.7 while the Van Genuchten (1980) method was used to obtain that of the non-woven geotextile material. Initial suction value for RCS was set at a value corresponding to the volumetric water content at maximum dry density as obtained in the laboratory soil tests. The defined materials were then allocated to their corresponding defined regions.

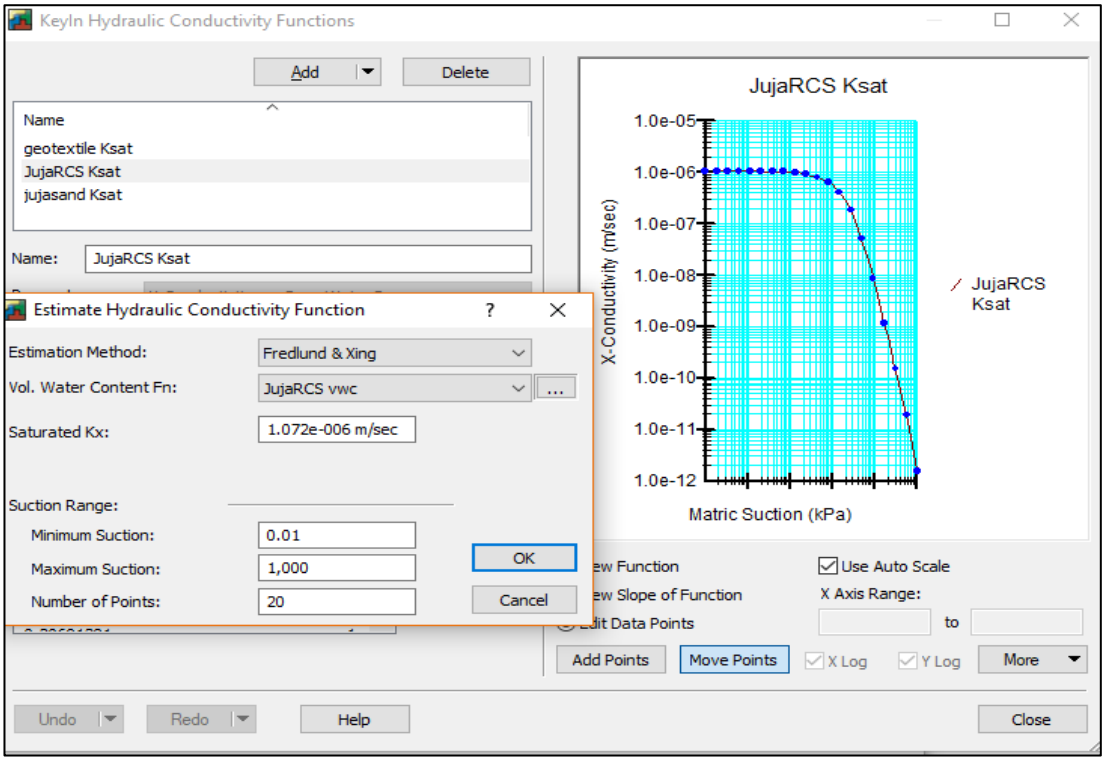

Figure 3.7: Estimation of the Hydraulic conductivity function of the RCS in SEEP/W

Keying in the boundary conditions and allocating them to the respective areas is the next step after assigning materials to their regions. Boundary conditions for the slope and top flat region corresponded to a rainfall event as obtained from the meteorological department of Kenya.

In the specification of the boundary conditions of the embankments, Rainfall data obtained from the meteorological department was used to specify the conditions of the simulated embankment. A rainfall event of 160mm/day with an exceedance probability of 5% was reported as heavy rainfall from the meteorological department of Kenya. Rainfall of such magnitude within the Nairobi region in most occasion occurs for a maximum period of two days. However in this research, rainfall on the embankment was simulated for a period of three days. This rainfall was applied to the top as a unit flux $1.85 \times 10^{-6} m/s$ and sloping side $1.062 \times 10^{-6} m/s$ of the embankment with the bottom part of the embankment having a zero flux.

The bottom of the embankment region was assigned a zero flux. Mesh configuration was the final step in which the quad and triangles mesh configuration of elements of height 0.1m as obtained in the calibration and validation was used in the study.

Stability modelling procedure in SLOPE/W

After the modelling in SEEP/W the results of the simulations were imported to SLOPE/W for stability analysis. In the stability analysis the material strength parameters are required and were keyed in as illustrated in Figure 3.8. The effective cohesion of the RCS was set to 0 kPa as is the practice in the design using cohesive soils (Berg et al., 2009).

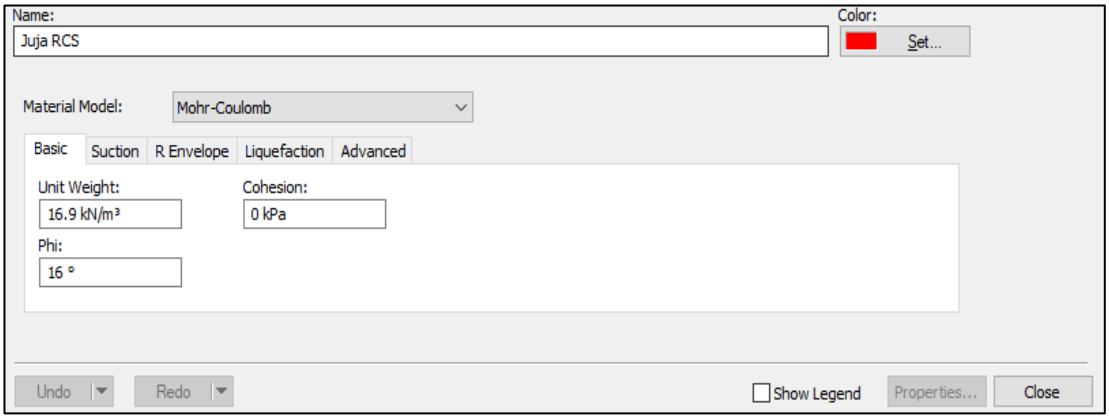

Figure 3.8: RCS materials properties in SLOPE/W

The non-woven geotextile material was keyed in as a reinforcement load with a tensile capacity of 21kN/m^2. The reinforcement load was assumed to be uniformly distributed throughout the depth. The geotextile layer was anchored to the RCS zone with the sand sandwiching the geotextile.

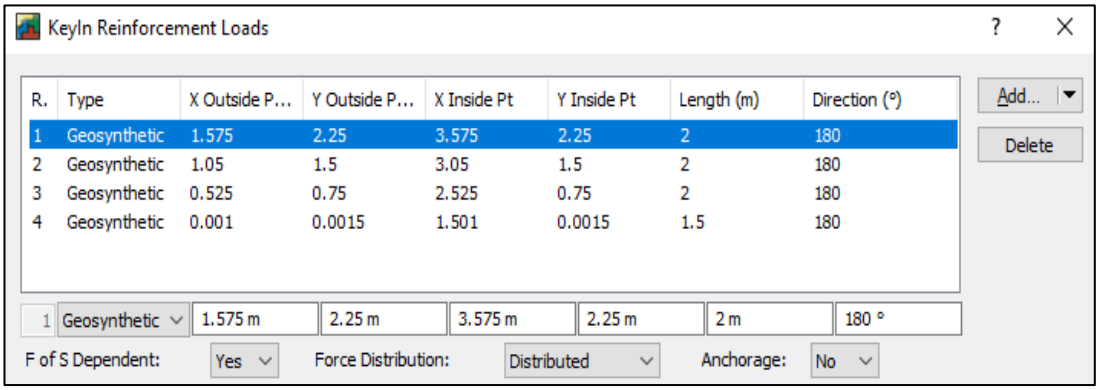

Figure 3.9: Keying-in of reinforcements loadings in SLOPE/W

In analysis, the Spencer method which satisfies all equilibrium conditions (i.e., moment equilibrium, vertical and horizontal forces) was selected in the SLOPE/W stability analysis with the "entry and exit" method specified for the failure circle .The entry points for the global stability were specified as between grids (2.1, 3) and (6, 2.6) while the exit points between grids (0, 0) and (2.1, 3) as can be illustrated in Figure 3.11. In the local stability study the entry point of the failure circle was specified

between the grids (2.1, 3) and (6, 2.6) while the exit points specified were between (1.575, 2.25) and (2.1, 3)

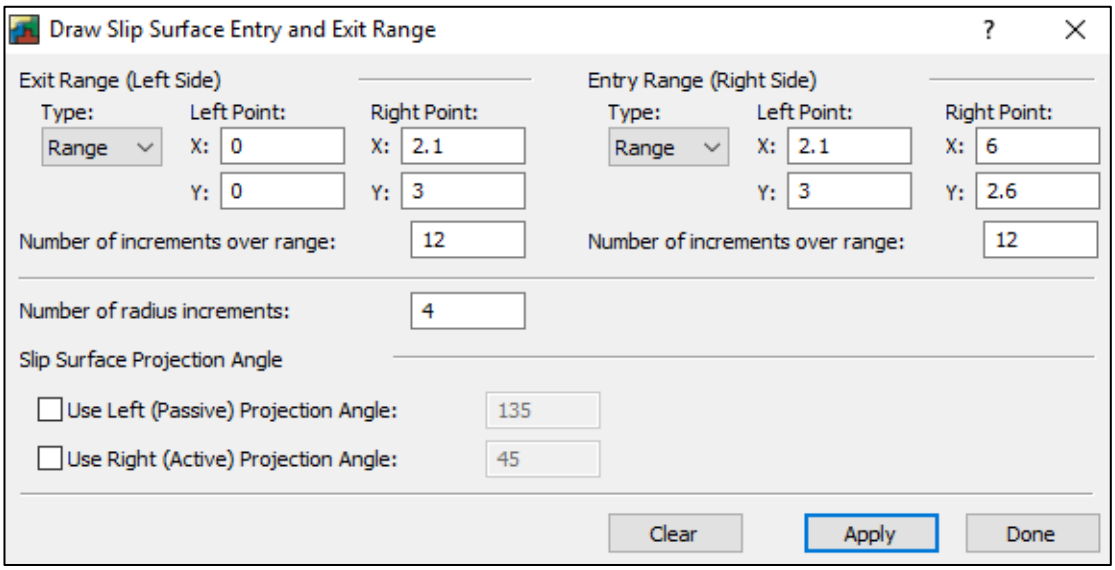

Figure 3.10: Entry and Exit range specifications in SLOPE/W for global stability analysis

Using the above procedure the shear strength of the backfill soils in the embankment were determined using the Vanapalli (Equation 2.12.)

3.4.3 Effect of sand cushion thickness on drainage and stability of RCS embankments

With the optimum angle of inclination arrived at. Sand layers of different thickness were introduced to sandwich the non-woven geotextile layers. The numerical model set up is as shown in Figure 3.11

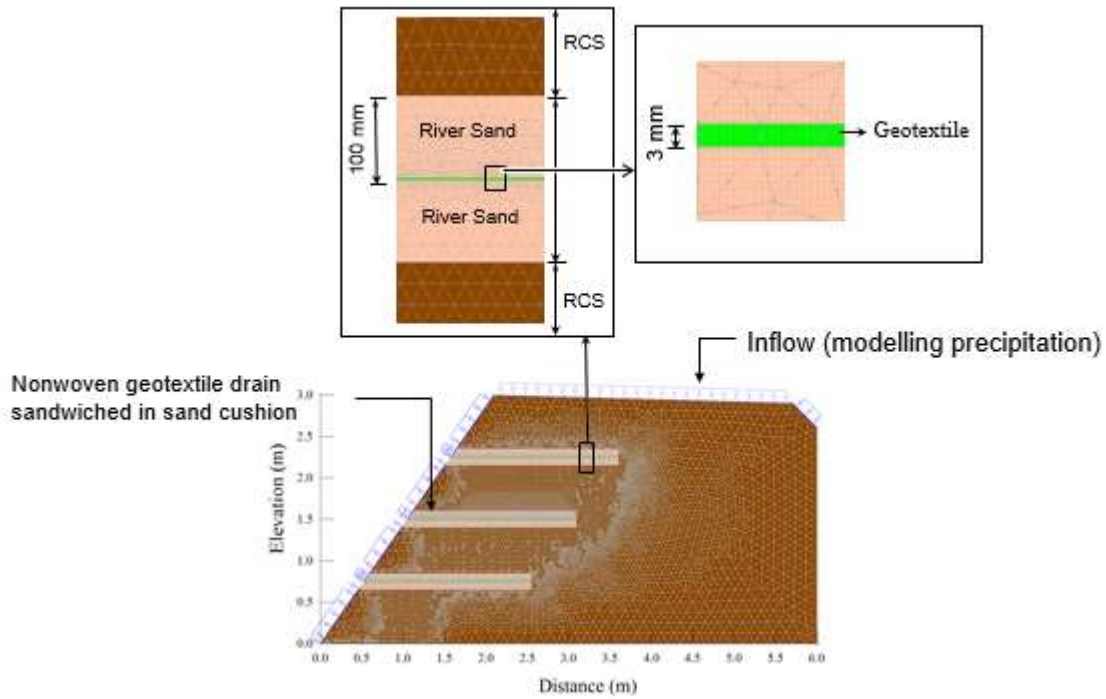

Figure 3.11: Numerical model set-up to investigating the effect of sand thickness on performance of RCS embankments

Properties of the river sand to be used were first determined in the laboratory using relevant ASTM standards. Sand properties of interest in the study included the specific gravity of the sand ASTM D854, (2014), sand gradation (ASTM D7928, 2017)., shear strength parameters conducted using the direct shear box method for the cohesionless soil (ASTM D3080, 2011) and hydraulic conductivity of the sand.

In the SEEP/W model a new region for sand that sandwiches the non-woven geotextile layer was introduced. Seven embankment models were simulated to reflect the 0mm, 50mm, 100mm, 150mm, 200mm, 250mm and 300mm thickness of the sand layers under study. The sand thickness layers corresponded to replacement of RCS by introduction of 0, 5, 10, 15, 20 and 25% of the volume of the embankment with sand. Properties of the sand layers in the model were defined using the same procedure earlier described for the RCS with the properties of the sand obtained from the

laboratory testing entered. The Fredlund &Xing model function was used to describe the hydraulic conductivity function of the sand.

In the stability simulations the shear strength parameter of the sand were defined as shown in Figure 3.12

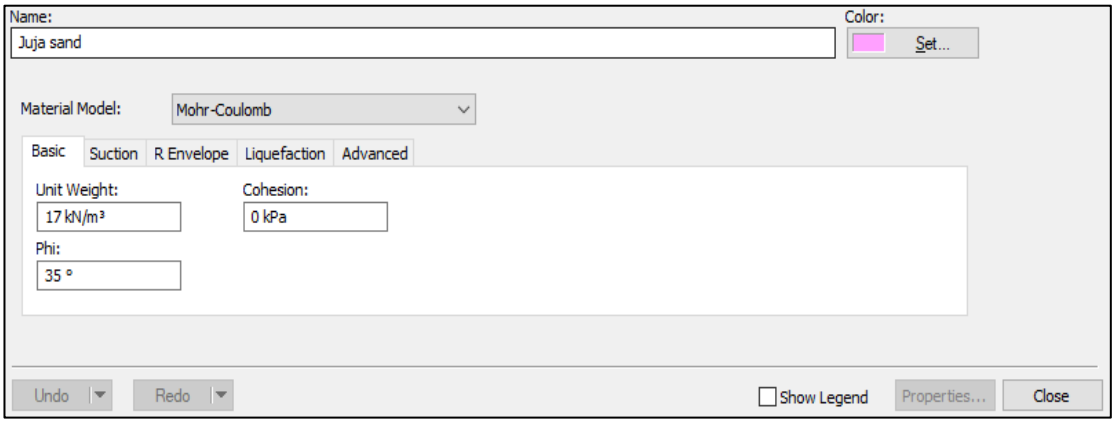

Figure 3.12: Shear strength parameters of River sand

In the stability simulations both the local and global stabilities of the embankments were investigated. For the local stability the entry and exit of the failure plane were described as shown in Figure 3.13.

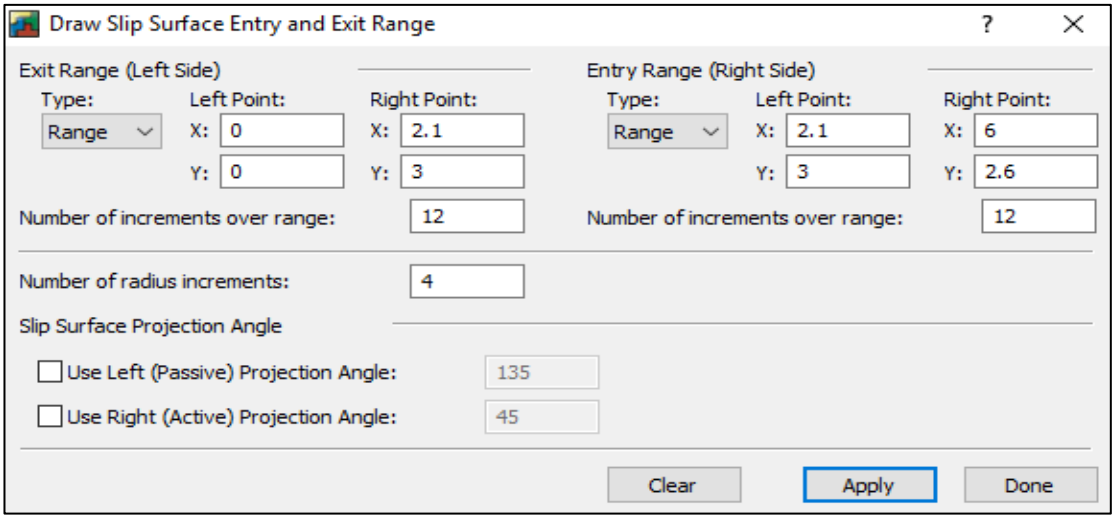

Figure 3.13: Entry and exit method of slip surface definition in SEEP/W

3.4.4 Effect of drainage layers spacing on the drainage and stability of RCS embankments

In the evaluation of the effect of the drainage layer spacing on performance of the RCS embankments, the embankment with 100mm thick sand layer on either side of the geotextile spaced at 0.75m was used. Three similar embankments were simulated though with the drainage layer spacing now adjusted to 0.25m, 0.5m and 1m. Boundary conditions for the transient analysis were rainfall event for the sloping side and the upper surface of the embankment with zero flux for the bottom. A transient analysis to determine the pore-water distribution in the embankments was conducted. Stability analysis was conducted with a similar procedure as in Section 3.4.3. The local and global stabilities of the embankment were evaluated. Exit points in the local factors of safety evaluation were adjusted to match the locations of the locations of the non-woven geotextile layers in the embankments (i.e. the exit points for the 0.25m and 0.5m drainage layers spacing were (1.75, 2.5) and (2.1, 3) while that for the 1.0m spacing was (1.4, 2) and (2.1, 3).

Data analysis

Data analysis in the seepage analysis included the determination of pore-water pressure measured along the vertical lines x=1.2m and 2.4m. The pore-water profiles of the embankments were determined and compared. Embankments with low pore-water pressure profiles within them are the best performing embankments as higher pore-water pressures in embankments contribute to the decline in the strength of the soil backfills. Stability simulations were analysed by comparing the trend in the factors of safety of the embankments. High factors of safety above 1 show the embankment is stable while lower values below 1 signify the failure of the embankment.

CHAPTER FOUR

RESULTS AND DISCUSSION

4.1 Introduction

The main objective of this research was to investigate the effects that the drainage layer configuration has on the moisture distribution and stability of reinforced RCS embankments. Specifically, the effect of the thickness, angle of inclination and spacing of the drainage layer were investigated. This chapter presents the results and appropriate discussions of the research objectives and the properties of the materials used in the study.

4.2 Modelling infiltration in unsaturated soils backfill using SEEP/W

4.2.1 Model Calibration

In the calibration of the numerical model SEEP/W. A numerical embankment to simulate infiltration of unsaturated backfill embankments as reported by Iryo & Rowe,(2005) were used. Comparison of the moisture distributions in the embankment and the numerical models simulations with varying element configurations are as presented in the Figure 4.1

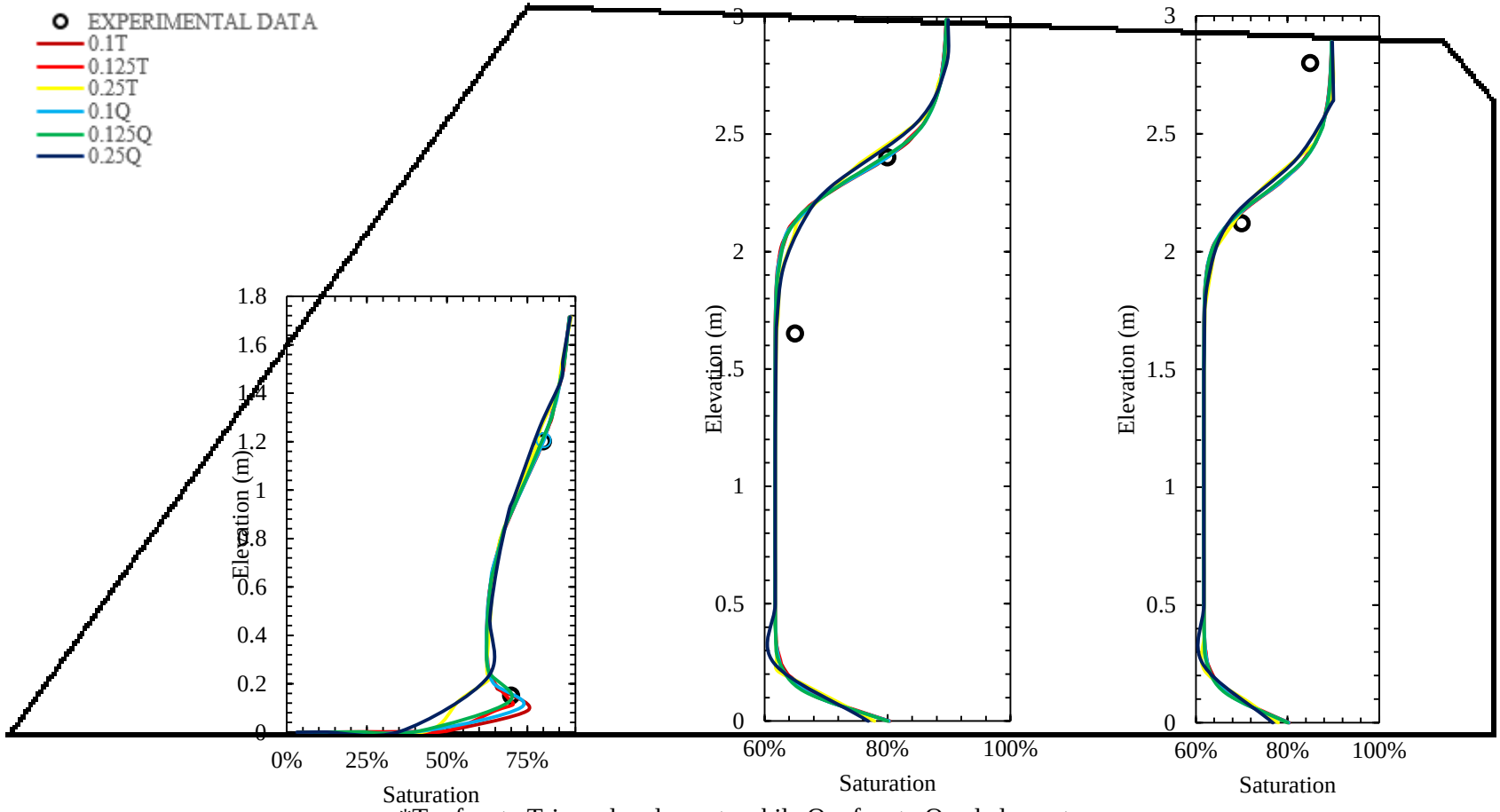

*T refers to Triangular elements while Q refers to Quad elements

Figure 4.1: Moisture distribution in the simulated Embankment model at locations x=1.2m, 2.4m and 4.8m from the toe of the embankment

From the results there seems to be a good relationship in trend between the simulated and the experimental results. The smaller elements configurations are seen to predict the moisture distribution better. The models results were compared to the experimental results and the coefficient of determination for the different element configurations as obtained from Ms Excel summarised in Table 4.1.

Table 4.1: Coefficients of determination for the different elements configurations in the embankment

Elements configurations	0.1T[a]	0.125T	0.25T	0.1Q[b]	0.125Q	0.25Q
R^2	**0.815**	**0.709**	**0.760**	**0.828**	**0.821**	**0.748**
RMSE	**0.051**	**0.059**	**0.067**	**0.047**	**0.048**	**0.073**

[a] 0.1T refers to Triangular elements of height 0.1m.
[b] 0.1Q refers to Quad elements of height 0.1m.

Acceptability of the element configuration was based on how close to 1 the coefficient of determination (R^2) were and how low the RMSE value was. A good fit was obtained from the modelled results with the coefficient of determination of the model varying from 0.709 to 0.828 and RMSE value ranging from 0.047 to 0.073. The quadrilateral elements produced better results as compared to the triangular elements which was in agreement with the recommendations of GEO-SLOPE International, (2010). However a mesh configuration of 0.1 with quad elements recorded the highest coefficient of determination 0.828 and lowest RMSE value of 0.047 compared to the other element size and shapes. The model could not achieve high precision values. This is attributed to hysteresis nature of the unsaturated soil as SEEP/W employs the use of only the wetting curve unlike in the experimental setup where both the wetting and drying water retention curves exists. The element configuration of quadrilateral elements of 0.1m height were adopted to verify the suitability of the model in the validation stage.

4.2.2 Numerical model validation

With the model calibration arriving at mesh configuration of quad elements of height of 0.1m the validation of the model was carried out using two other reinforced embankments. Figure 4.2 shows the comparison of the experimental and the predicted water content. The data measurements were taken vertically at point x=1.2m, 2.4m and 4.8m. The peak in the graph represented the points where the non-woven geotextile layers were located and the peaks represent low water levels in the geotextile layers. This is attributed to the drainage power of the non-woven geotextile layers.

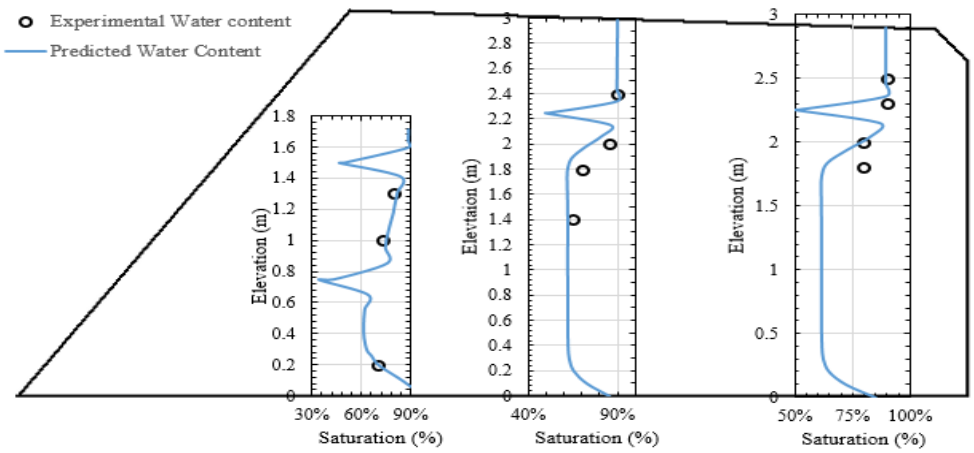

Figure 4.2: Water content distribution in Embankment 2

A correlation analysis on the experimental and the predicted saturation levels were conducted and a 0.7644 value was obtained as shown in Figure 4.3.

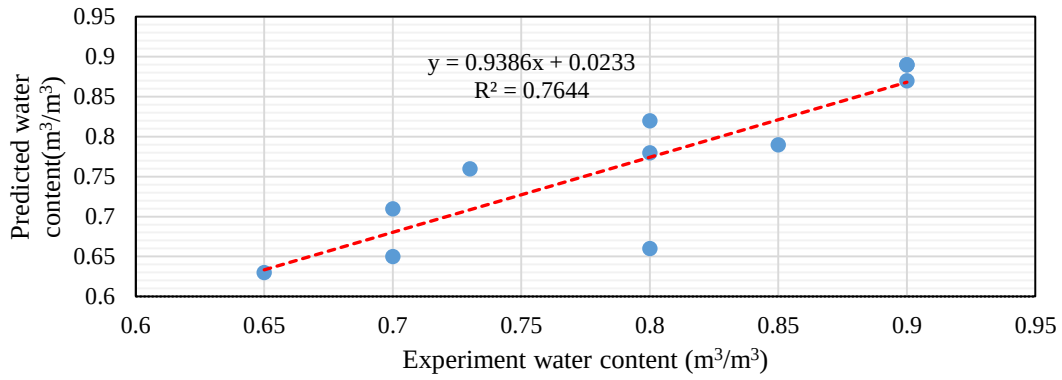

Figure 4.3: Relationship between the predicted and experimental water content in embankment 2

The validation was done on one more embankment with unequal non-woven geotextile labelled embankment three and the saturations level in the embankment are as presented in Figure 4.4 .

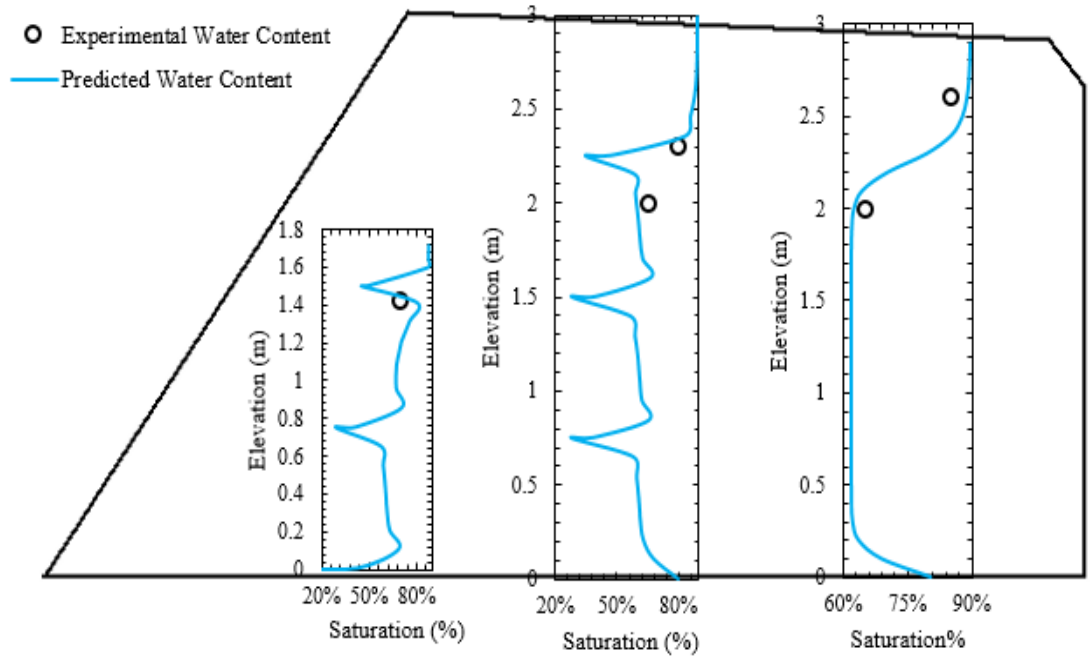

Figure 4.4: Water content distribution in Embankment 3

Results from numerical simulations showed a similar trend with the experimental results, which suggested the numerical simulation can simulate infiltration in unsaturated soil nonwoven geotextile systems. The use of the non-woven geotextile as a drainage layer was well simulated as shown by a decrease in the saturation levels in the areas where the non-woven geotextile layers were located. Areas occupied by the sand zone recorded higher water content levels due to a reduced hydraulic conductivity compared to the non-woven geotextile layer. The coefficient of determination though consistent (0.76 in embankment 2) in the two embankments had a slight decline from that in the calibration, this was attributed to the clogging of the non-woven geotextile layer with fine particles from the sand backfill which could not be simulated. The

difference between the measured and predicted values similar to the earlier embankment results are due to hysteresis nature of hydraulic characteristic of unsaturated soil.

Similar observations on suitability of numerical model SEEP/W in simulating infiltration has been reported by a number of researchers (Maula & Zhang, 2011; Thuo, Yang, & Huang, 2015; Xue, Ajmera, Tiwari, & Hu, 2016; Yang et al., 2017). Accordingly, quadrilateral elements of height 0.1m with six linear time steps were found adequate and thus adopted for the study.

4.3 Effect of Non-Woven Geotextile Layers Inclination on the Drainage and Stability of RCS Embankments

4.3.1 Materials properties

RCS was collected at a moisture content of 38.15% and this was attributed to the wet weather during the time of the soil collection.

Specific gravity of soil is important property in its classification and derivation of other soil properties which include void ratio, porosity and unit weight. Set of three tests were done for each of the soil sample. RCS recorded a specific gravity of 2.58 reported at a temperature of 20°C. Denge, (2017) reported a specific gravity of the RCS at 2.52 a value which is within range to the one obtained in our results.

The gradation test was done to establish the particles size distribution in the test sample. From the laboratory tests RCS was established to be sandy silty clay with traces of gravel. Silt which includes particles of diameter between 0.002mm to 0.075mm as shown in Table 4.2 was dominant in the soil at 51.85%.

Table 4.2: Percentage RCS soil components

Classification	Clay	Silt	Sand			Gravel
			Fine	Medium	Coarse	
Sieve size (mm)	<0.002	0.002-0.075	0.075-0.425	0.425-2	2.00-4.75	>4.75
Percentage	38.5%	51.85%	5.12%	3.55%	0.78%	0.2%

The particles distribution curve for the RCS is as shown in the Figure 4.5. The curve constitutes of results obtained from both the wet sieve analysis and hydrometer test. The figure shows that 90% of the RCS passes through the 0.075mm sieve which comprises of the silts and clays. For the recommendations of AASHTO 2009 to apply in the design of walls and embankments the backfill material should have marginal material (soil passing the 0.075mm sieve) less than 35%. Red coffee soil as backfill material does not fulfil the condition thus special emphasis on the drainage aspect of the embankment to ensure stability has to be considered as recommended from studies by Berg et al., (2009).

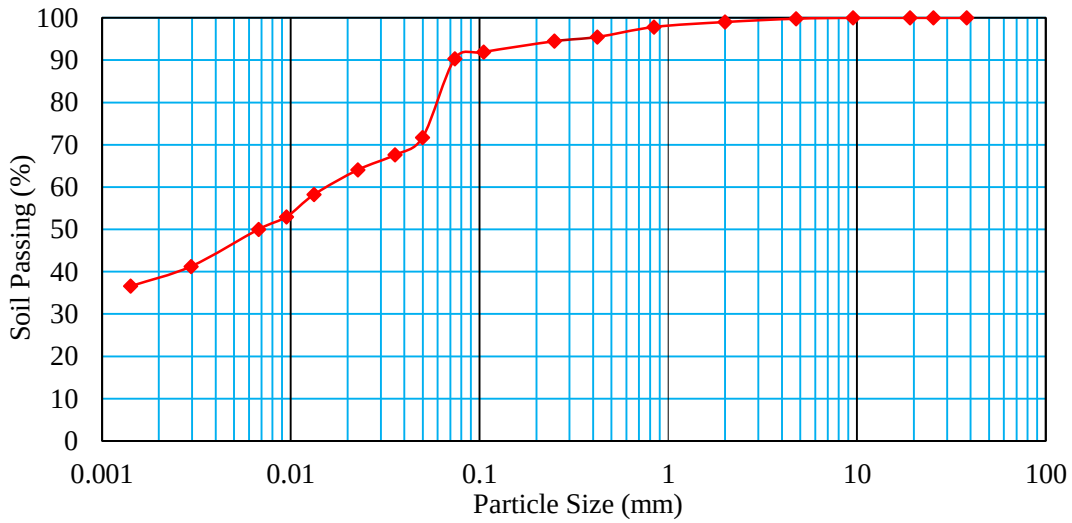

Figure 4.5: Gradation curves for red coffee soils

The atterberg limits for the RCS was done based on ASTM D4318. Atterberg limits determine the state of the soil at different moisture content values. From the laboratory

tests carried out the liquid limit , plastic limit and linear shrinkage values were obtained as 48.8%, 27.0% and 15.2% respectively. The liquid limit was obtained from Figure 4.6 and is the water content corresponding to 20mm penetration. Plasticity index of the RCS which is the difference between the liquid and plastic limit was obtained as 21.8%. Plasticity index denotes the range of water content the soil exhibits plastic properties. The value of 21.8% is classified as low plasticity according to ASTM D4943. With the liquid limit , plasticity index and particle size distribution of the RCS obtained the soil was classified as low plasticity silty clay (CL) according to the Unified Soil Classification System (USCS).

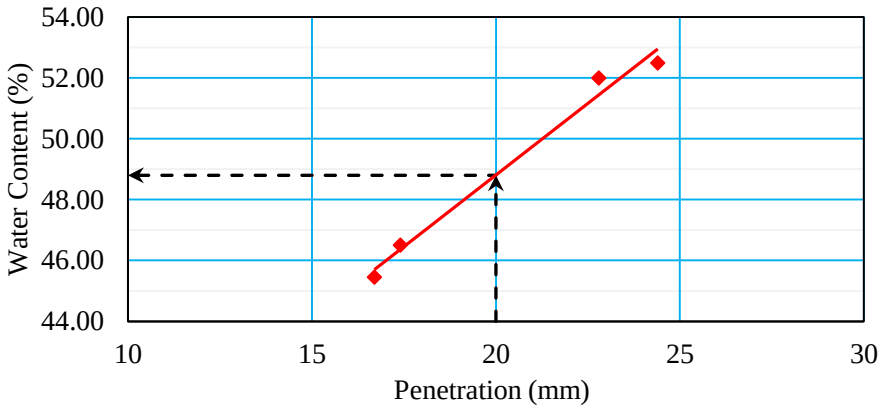

Figure 4.6: Liquid Limit Cone-penetrometer method

Similar laboratory tests on the atterberg limits of the RCS of Juja by (Denge, 2017; Njike et al., 2014) reported a liquid limit value of 48% with Denge,(2017) reporting a plastic limit of 30.4% and (Njike et al., 2014) reporting 25%.

The standard compaction test is used to determine the maximum dry density (MDD) and optimum moisture content (OMC) of the RCS. Five tests were run and corresponding moisture content and dry density of the RCS plotted. The results are as represented in Figure 4.7. An optimum moisture content of 26.2% and maximum dry density of 1337Kg/m^3 obtained.

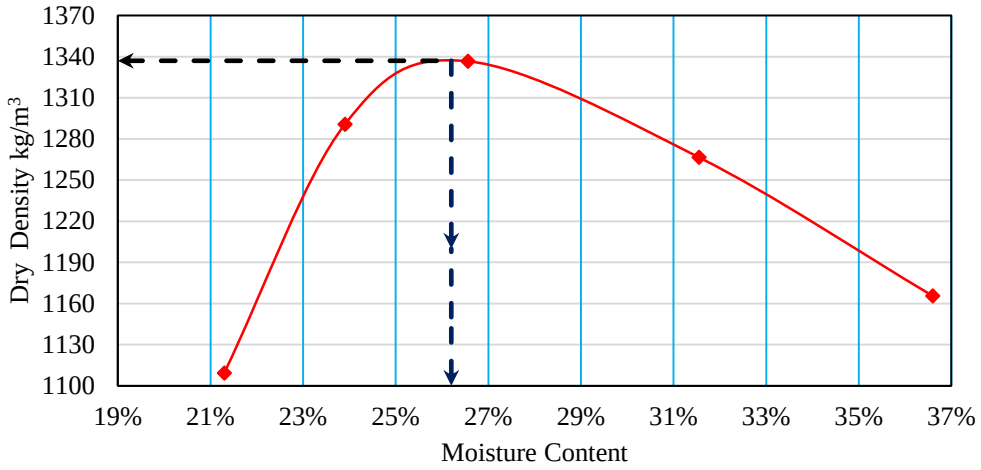

Figure 4.7: Compaction Test Curve

The consolidated undrained triaxial test was carried out to determine the shear parameters of the RCS. Samples remoulded to the maximum dry density and optimum moisture content were used for this test. Mohr circles are shown in Figure 4.8. From the Figure the total cohesion (c) of the red coffee soil obtained from the intercept of the total failure envelope on the shear traction axis was obtained as 22kPa while the total soil friction angle (φ) which corresponds to the slope of the total failure envelope in the Figure 4.8 is 17°. The effective cohesion (c') of the red coffee was obtained as 32kPa while the effective soil friction angle (φ') which corresponds to the slope of the effective failure envelope is 16°. In the design of embankments and walls the total values of the shear strength parameters are used in the design of temporary structures while the effective which takes into consideration the loss of pore pressure in the soils are used in the design of structures that have a long design life. This study adopted the effective strength parameters.

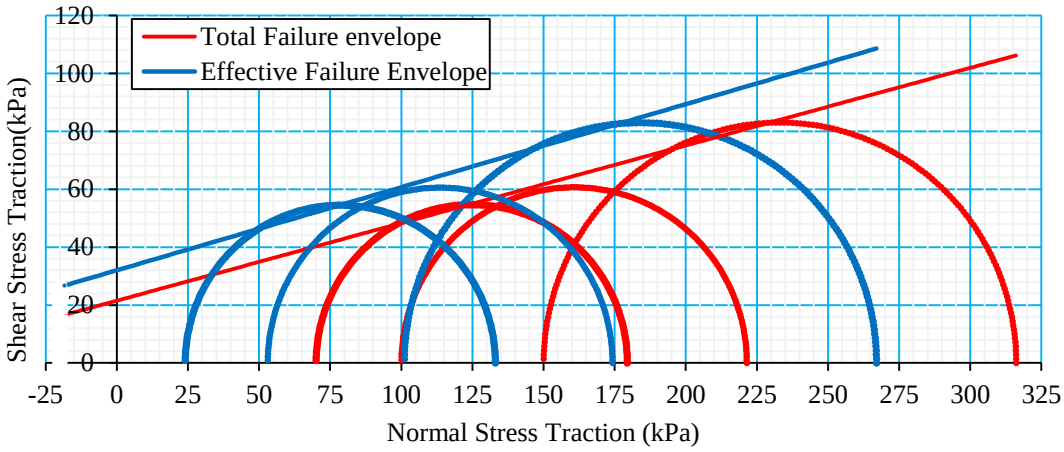

Figure 4.8: Total and effective stress Mohr circles of RCS

Table 4.3 below summarizes the properties of the RCS as obtained in the laboratory tests

Table 4.3: Summary Red Coffee Soils properties

Properties	**Values**	**Measurement method**
Specific Gravity	2.58	
Particle size distribution		Sieve and Hydrometer
Gravel	0.2%	
Sand	9.45%	
Silt	51.85%	
Clay	38.5%	
Atterberg limits		
Liquid limit	48.8%	Cone Penetrometer
Plastic limit	27.0%	
Plastic Index	21.8%	
Type of soil	CL	USCS
Hydraulic Conductivity	$1.072 \times 10^{-6} cm/s$	Falling Head permeability
Optimum Moisture content	26%	Standard Compression Test
Maximum Dry Density	1337 Kg/m^3	Standard Compression Test
Effective Cohesion C'	32kPa	CU Triaxial
Effective Friction angle φ'	16°	CU Triaxial

The properties of the non-woven geotextile were obtained from the secondary sources (Iryo & Rowe, 2005) values which conformed to the typical tensile strength of non-

woven geosynthetics in the market as also reported by Shukla et al., (2011). The properties of the non-woven geotextile materials used in the study are as summarized in Table 4.4.

Table 4.4: Properties on the non-woven geotextile materials as reported by Iryo and Rowe (2005)

Mass per unit area, m_a (g/m^2)	310
Thickness of geotextile, $t_{geotextile}$ (mm)	3
Porosity, n_p	0.92
Saturated hydraulic conductivity in plan direction, $k_{sat\ geotextile\ plane}$ (m/s)	$2.3x10^{-2}$
Saturated hydraulic conductivity in cross plane direction, $k_{sat\ geotextile\ cross}$ (m/s)	$3.5x10^{-3}$
Tensile strength in machine direction (kN/m)	21.6

From the properties of the materials obtained from laboratory tests, the volumetric water content function of RCS and non-woven geotextile and the hydraulic conductivity function in relation to matric suction were determined. This was achieved through the 'sample function' method in SEEP/W. Sample function, "silty clay" for the RCS and "sand" for the geotextile material. The volumetric water content function is as shown in Figure 4.9.

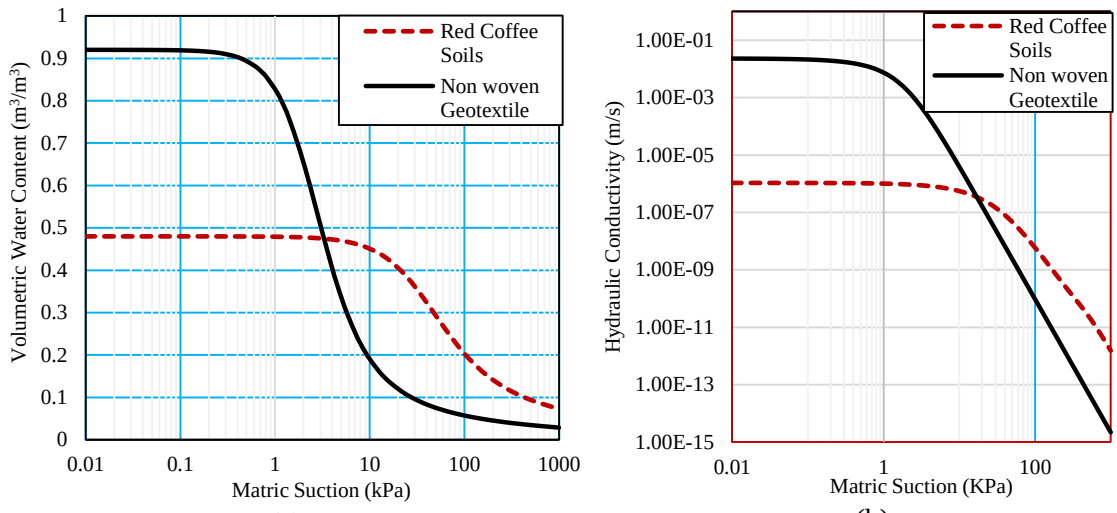

Figure 4.9: Hydraulic functions of the RCS and the non-woven geotextile

From the graphs matric suction is observed to be influenced by the volumetric water content of geomaterial. It can be observed that as the volumetric water content of the soils increases matric suction significantly decreases which is in agreement with soil mechanics principles in which soils with high volumetric water content will exert a lower pressure in moving water towards them as compared to dry soils. An important component in the functions is the air entry value which shows the point at which matric suction is adequate to initiate the dying of a saturated soil. RCS has a higher air entry value 15kPa compared to that of non-woven geotextile which stands at 0.9kPa. This is because the amount of flow paths within non-woven geotextile is more flow paths thus a lower pressure is required for water movement as compared to RCS with finer particles and lesser flow paths. The curve of the geotextile are steeper showing water is lost at a much faster rate in these geomaterial as compared to RCS. These observations conform to the study by Lu et al., (2006) which showed that soils with a relatively wider pore-size distribution are marked by relatively less steep characteristic curves because the majority of pores are drained over a relatively wider range of suction.

4.3.2 Pore-water Pressure profiles

Figure 4.10 shows the pore-water profiles of the RCS slopes with different non-woven geotextile angle of inclination at the end of days 1, 2 and 3 of the rainfall event. There was a significant development of pore-water pressure in the embankments during the rainfall event. Throughout the rainfall event pore-water pressure steadily increased as the rainfall flux infiltrated through the embankment. Matric suction dissipation was observed as pore pressure build up was recorded where the rainfall flux passed. With an initial matric suction of -60kPa at the beginning of the rainfall, RCS recorded positive pore-water pressure values on the third day at the base of the embankment a distance x=1.2m and x=2.4m from the toe. In Figure 4.10 (c and f) further demonstrate the advantage of provision of a non-woven geotextile at the base of the embankment in embankments exposed to long term rainfall durations. As can be observed, the embankments in which drainage layers were provided had low pore-water pressure values signifying better drainage which ultimately contributed to a higher soil strength and stability.

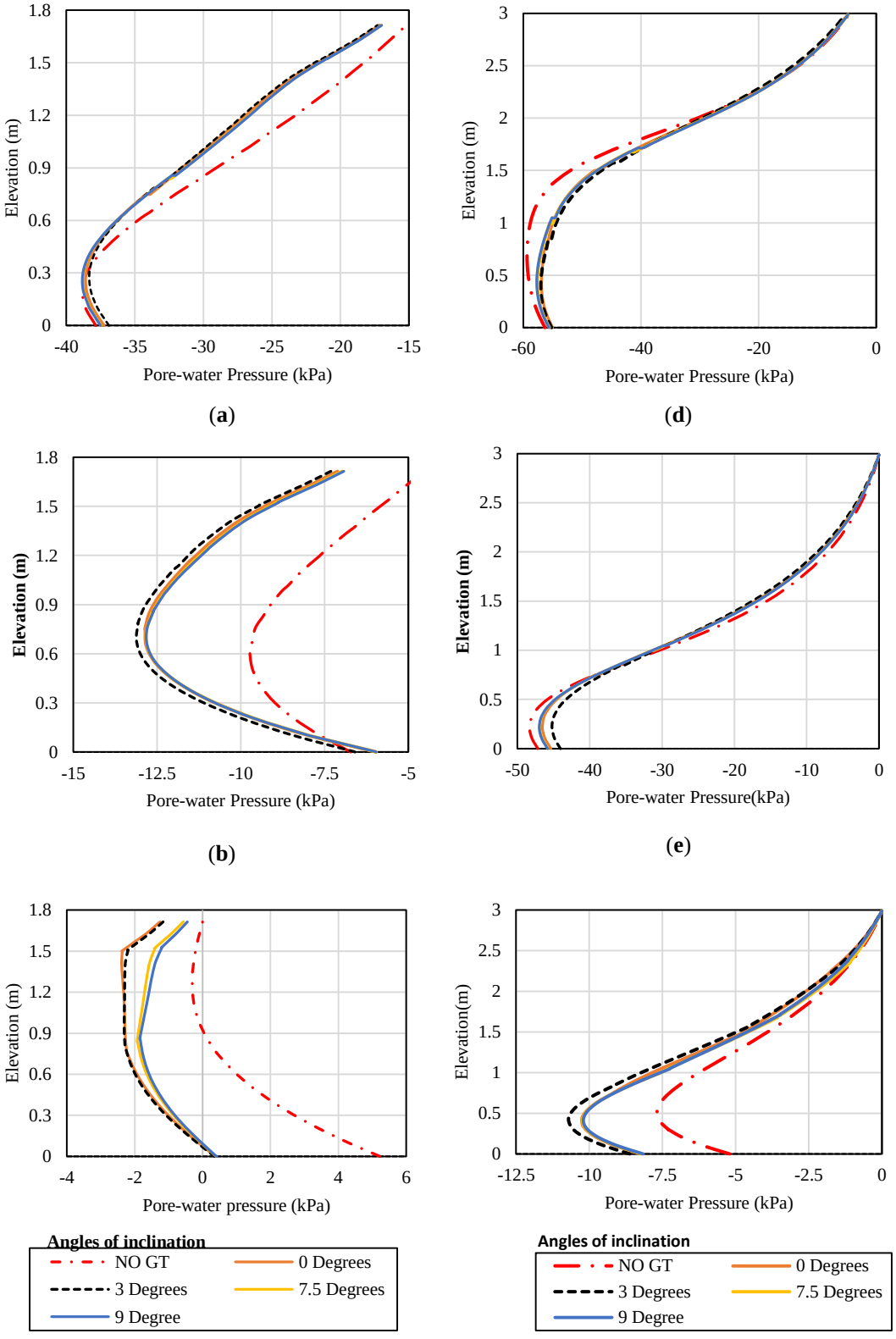

Figure 4.10: Pore-water pressure profiles at (a) x=1.2m day 1 (b) x=1.2m day 2 (c) x=1.2m day 3 (e) x=2.4 day 1 (e) x=2.4 m day 2 (f) x=2.4m day 3

From the Figure 4.10, it is clear that inclining the non-woven geotextile layer has an effect on the pore-water pressure distribution in the embankment. Increasing the non-woven geotextile angle of inclination from the conservative angle of zero degree upto an angle of three degrees resulted in the reduction of the rate of pore-water pressure development in the embankment. However increase of the inclination angle beyond three degrees did not yield any further improvement in the pore-water pressure development. This is attributed to the drainage that occurs when the non-woven geotextile layers are inclined. When the non-woven geotextile layers are inclined the water that was accumulating on the soil layer just above the non-woven geotextile begins to move through the slope created unlike in the zero degrees angle of inclination where water accumulated upto saturation before moving into the geotextile layer. This conforms to the Darcy equations of groundwater flow in which the quantity of water flow is directly proportional to the loss in head over a length as shown in Equation 4.1.

$$q = KA\frac{h_l}{L} \quad \textbf{(4.1)}$$

Where: q is the flow rate through the soil layer; A is the area of the pathways available for water movement; h_l is the head loss over the horizontal length and L is the horizontal length.

In the event where the geotextile layer was horizontally placed at zero degrees the head loss in the horizontal aspect was tending towards zero thus there was limited flow out of the embankment. However when the geotextile layer was inclined an appropriate change in head was introduced thus improved water flow above the geotextile layer. This clearly demonstrates that inclining the non-woven geotextile material brings the advantage of early drainage. Three degrees angle of inclination was determined to be

the optimum angle for effective drainage in the RCS embankments. Similar results on the improvement of drainage by inclining geotextile have been reported by researchers (Iryo & Rowe, 2005; Nishigaki, M., Umeda, & Kono, 1993).

It was also be observed that in the early stages of the rainfall event, the embankments with non-woven geotextile material recorded higher rates of pore-water pressures within its profiles as compared to the embankment with no reinforcements as in Figure 4.11. This is attributed to the capillary barrier which contributed to water accumulation above layers of the non-woven geotextile.

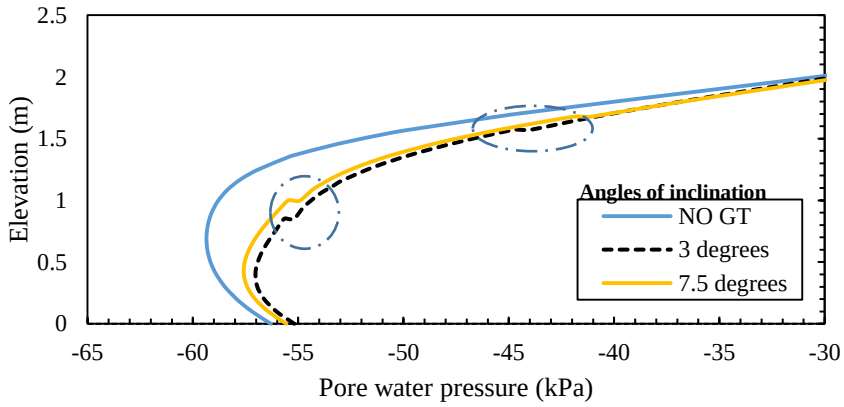

Figure 4.11: Pore-water pressure development above the non-woven geotextile layers

4.3.3 Embankments' stability

Figure 4.12 shows the variation of the minimum factors of safety with change in geotextile inclination angles. There is a general decrease in factor of safety of the embankment with increase in accumulated rainfall. Initially the factor of safety of the reinforced embankments had minimal changes to that of the unreinforced embankment. This can be attributed to the accumulation of water above the top most non-woven geotextile layers in the early stages of the rainfall event a phenomena referred to as capillary barrier. The accumulation of water above the top most non-woven geotextile layer, effectively led to the development of pore water pressure and

a subsequent reduction in the matric suction of the RCS in these regions. The accumulation of water has been reported to continue until the soil layer just above the non-woven geotextile becomes saturated (Albino & Portelinha, 2017; Yang et al., 2017). An increase in the pore water pressures above the non-woven geotextile layers due to water accumulation led to the reduction of the shear strength of the soils which contributed to the initial low factors of safety. However, with time as the rainfall flux passed through the RCS zone the regions above the geotextile became saturated this allowed the accumulated water to transit into the non-woven geotextile layer. The non-woven geotextile material now acted as drainage layer, dissipating pore-water pressure and thus record higher factor of safety values compared to the unreinforced embankment.

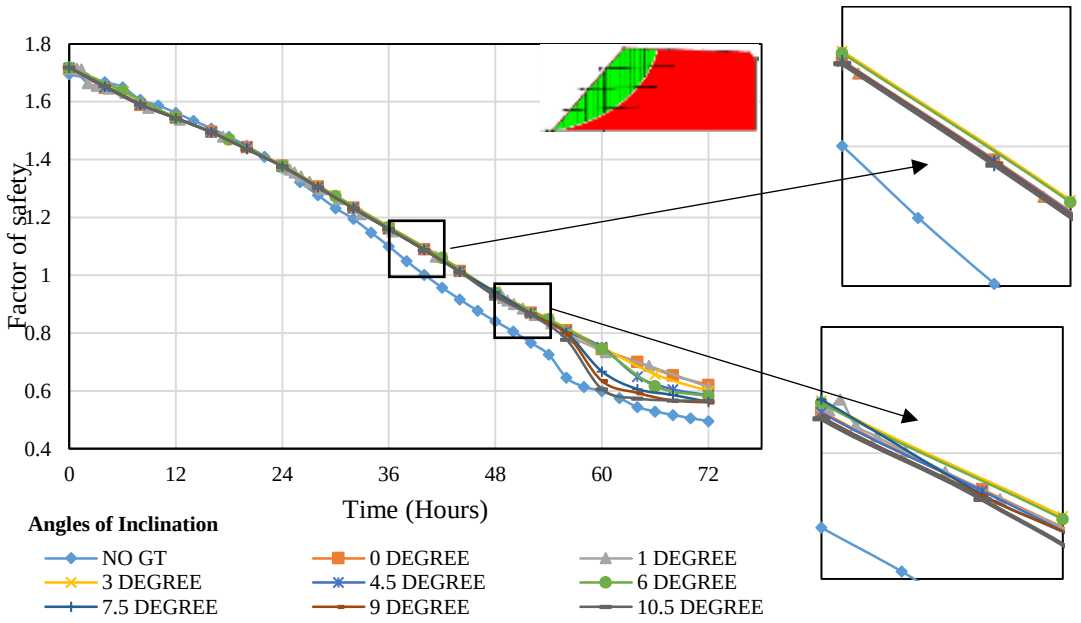

Figure 4.12: Variation of global factors of safety with change in inclination angle

It was also noted that with increase in angle of inclination, there was a slight improvement in the factor of safety. A one degree angle of inclination from the conservative zero degree increased the factor of safety of the embankment at the end

of 48 hours from 0.923 to 0.941 signifying a 2% increase in the factor of safety of the RCS embankment, while a three degree inclination improved the factor of safety to 0.969 giving an improvement in the factor of safety by 5%. Further increase in the angle of inclination did not significantly improve on the global factor of safety of the embankment. This as earlier explained in the pore water pressure profile section can be attributed to an improvement in the drainage aspect with part of the water above the non-woven geotextile flowing out of the embankment when the geotextile material is inclined. With improved drainage the pore water pressure that had developed due to water accumulation is dissipated to an extent. Referring to the Vanapalli equation (Equation 2.12) dissipation of the pore water pressure of the soil increases the matric suction and improves on the shear strength of the soil ultimately improving on the factors of safety as is illustrated in the Figure 4.12. However, increase in the factor of safety of the embankment increased until a three degree angle rise beyond which there was no significant improvement in the factors of safety of the embankment. A three degree angle was thus determined to be the optimum angle of inclination for drainage and improvement of stability in the RCS embankment. Iryo et al., (2005) reported an optimum angle of 10% in sand backfill which translates to a 3.5° inclination angle and does not deviate much from the results obtained of 3 degrees in this study.

4.4 Effect of Sand Cushion Thickness on Drainage and Stability of RCS Embankment

4.4.1 Materials properties

In addition to the properties of the RCS, the properties of river sand were obtained from laboratory tests. The specific gravity for the river sand was obtained as 2.68 with the saturated coefficient of hydraulic conductivity of 0.000013m/s. The shear strength angle of the river sand as obtained from the direct shear box were a frictional angle

of 35°. Sieve analysis was carried out and the gradation curve for the river sand is shown in the Figure 4.13. From the curve the diameter corresponding to 60% of the sand D_{60} was 0.62mm, D_{30} was 0.35mm and D_{10} was 0.15mm. Using the above values, the coefficient of uniformity of 4.133 and coefficient of curvature of 1.32 the sand was classified as poorly graded sand (SP), using the Unified Soil Classification System (USCS)

$$\text{Coefficient of uniformity}(C_u) = \frac{D_{60}}{D_{10}} = \frac{0.62}{0.15} = 4.133$$

$$\text{Coefficient of curvature } (C_C) = \frac{(D_{30})^2}{D_{60} \times D_{10}} = \frac{0.35^2}{0.62 \times 0.15} = 1.32$$

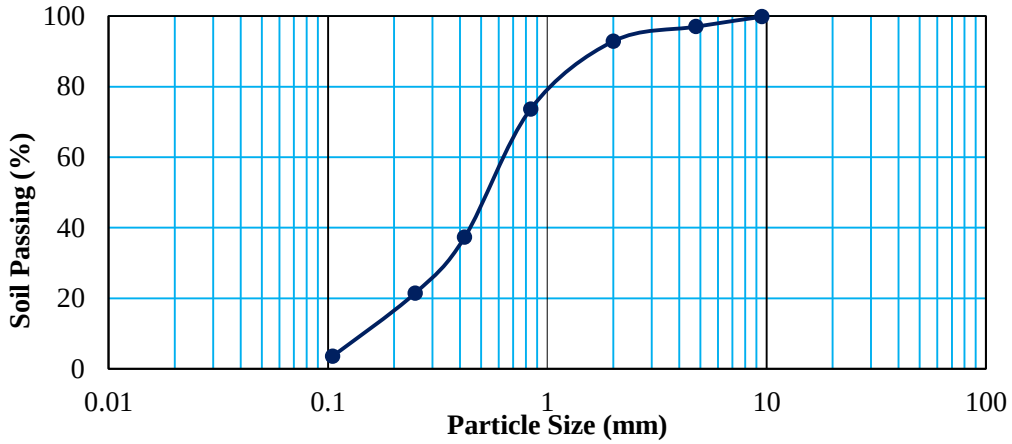

Figure 4.13: Gradation Curve for River sand

With the properties of the sand and the previously obtained RCS properties and non-woven geotextile properties the combined hydraulic function curves which now include the hydraulic functions of sand were incorporated as in Figure 4.14

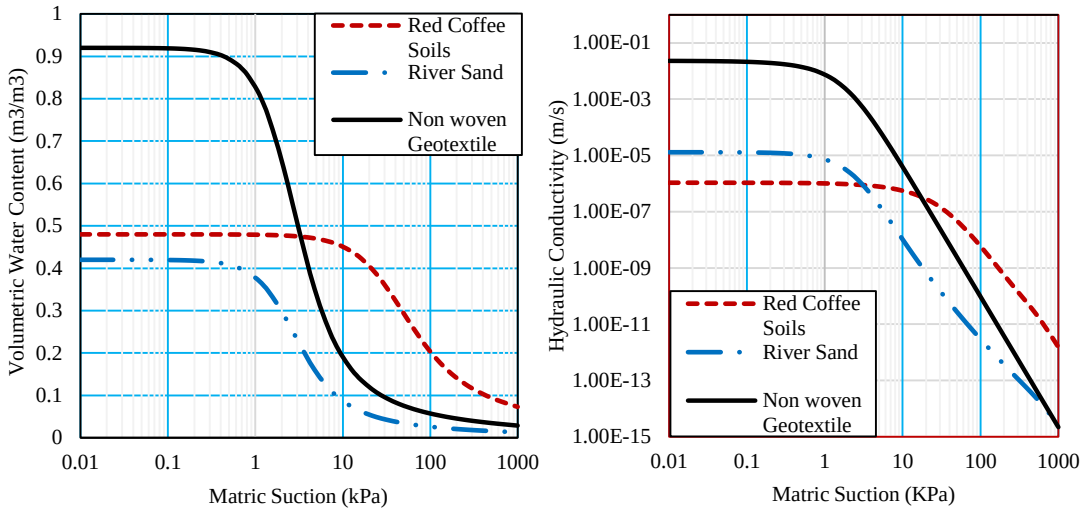

Figure 4.14: Hydraulic function models of river sand, non-woven geotextile and RCS

Figure 4.14 summarizes the hydraulic conductivity functions of the embankments backfill materials. The van Genuchten (1980) model was used to estimate the function for the non-woven geotextile from the parameters given by Iryo and Rowe (2005). The Fredlund and Xing's model was used to produce the hydraulic function of the RCS and river sand. Similar to the non-woven geotextile layer, sand soil had a lower air entry value of 0.9kPa as compared to that of the RCS. This as earlier discussed is attributed to an increase in the flow paths for soils with coarse particles, RCS made up of finer material has lesser flow paths thus more pressure is required to extract water from the neighbouring soils. The Figure 4.14b shows a decrease in hydraulic conductivity of the soils with increase in matric suction. The saturated hydraulic conductivity of the soils correspond to the lowest matric suction value of 0.01kPa. At a matric suction of 0.01kPa the hydraulic conductivity of river sand is higher compared to that of the river sand and RCS. This is because the flow in unsaturated backfill material is due to total hydraulic potential. The river sand with coarse grained materials loses water faster at a much faster rate as compared to the RCS with fine grained materials, this is attributed to the available pathways for water loss. RCS with finer

grain particles has less pathways available for water flow thus the conductivity levels of the soils are much lower. For the numerical analysis the initial matric suction values for the RCS was set at -60kPa to correspond to the OMC of 0.26 as obtained from the laboratory soil tests results while that for sand and the non-woven geotextile were set at -3.5kPa.

4.4.2 Pore-water pressure profiles

Figure 4.15 presents the pore-water pressure profiles of the embankments with varying sand cushion thickness. Pore-water pressure in the embankments is noted to increases with advancement of time and increase in cumulative rainfall this is because of the increase in the volumetric water content in the embankment with passage of time. Initially the embankment with non-woven geotextile not sandwiched between sand cushions layer performed better as characterised by lowest pore water pressure within its profile and a progressive increase in the pore water pressure development noted with increase in sand layer thickness, with embankment containing sand layers of 300mm recording the highest pore water pressure development. This is attributed to the difference in the initial matric suction of the sand and RCS in the embankment; because the loss of matric suction is attributed to the increase in the volumetric water content of the soil, RCS with a much lower hydraulic conductivity and high matric suction (60kPa) took a much longer time for the loss of matric suction and development of significant pore water pressure in the initial stages. On the other hand sand with a high hydraulic conductivity and low matric suction (3.5kPa) took much lesser time for pore water pressure development and this strongly explains the high pore water pressure values in the early stages of the rainfall event. The initial high pore-water pressure development rates in embankments with sand cushion was also

attributed to the fact that, part of the sand layers were exposed to the rainfall on the sloping part of the embankment. This made the sand layers to act as a medium through which rain water made its way into the embankment.

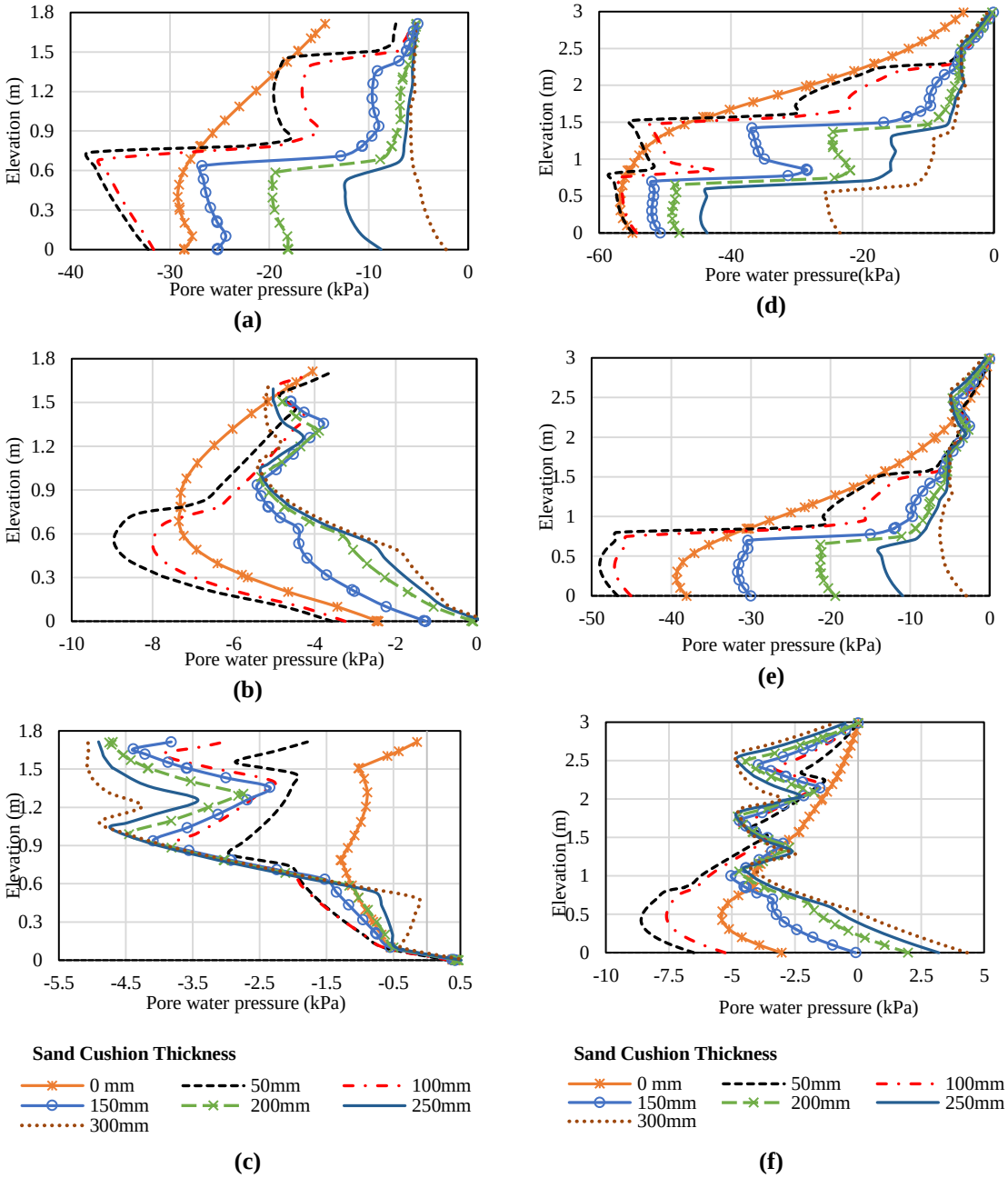

Figure 4.15: Pore-water profiles of embankments with change in sand layer thickness at end of: (a) day one x=1.2m from toe; (b) day two x=1.2m; (c) day three x=1.2m; (d) day one x=2.4m from toe (e) day two x=2.4m and (f) day three x=2.4m.

However with advancement of time RCS above the sand layers became saturated and the general volumetric water content in the embankment increased, this made the sand layers and non-woven geotextile material to act as drainage layers. Embankments with large sand layers had much improved drainage through its structure thus lower levels of pore-water pressure development as compared to similar embankments with thinner sand layers as can be seen in Figure 4.15 (c and f).

Sand layers have a high (0.000013cm/s) hydraulic conductivity as compared to that of the RCS ($1.072x10^{-6}$cm/s). Comparing the ratio of the rate of rainfall intensity ($1.85 \times 10^{-6} m/s$) to the hydraulic conductivity of the soils ($^{q}/_{k_s}$) values of the rainfall intensity to the river sand hydraulic conductivity gives a value of 0.142 while that of the rainfall intensity unit flux to that of the RCS gave a value of 17.2 . River sand with a ratio of less than 1 signifies that the river sand was not saturated throughout the rainfall event as the hydraulic conductivity of the sand was relatively high compared to the rate at which water infiltrated within it, thus river sand acted as a layer that drained water from the embankment layer. However in the case of RCS the hydraulic conductivity was very low leading to accumulation of water within the RCS layer. The introduction of the sand layers thus improved drainage and helped retard the rate of pore-water pressure development. It was generally observed that the pore-water dissipation increased with increase in sand cushion layer thickness. However a sand thickness layer from 150mm is determined to be adequate in the improvement of drainage in RCS embankments as is illustrated in the pore water pressure profiles of the various embankments.

Inclusion of sand cushions layers also helped minimise the development of capillary barrier above the non-woven geotextile material which is characterised by decreased pore water pressure values above the non-woven geotextile layers and helped improve drainage in marginal soils backfill. Thuo et al., (2015) arrived at similar results and reported the reduction of capillary barrier with the inclusion of thin sand cushion layers to sandwich the non-woven geotextile layers.

4.4.3 Local and Global stability

Figure 4.16 presents the variation of the local factors of safety of the embankment with change in sand cushion thickness. There is a general trend in decrease of the factors of safety with increase in time, this is due to increase in cumulative rainfall flux passing through the RCS embankment. Increase in cumulative rainfall leads to the decrease in the matric suction of the soil and reduces the strength of the soil.

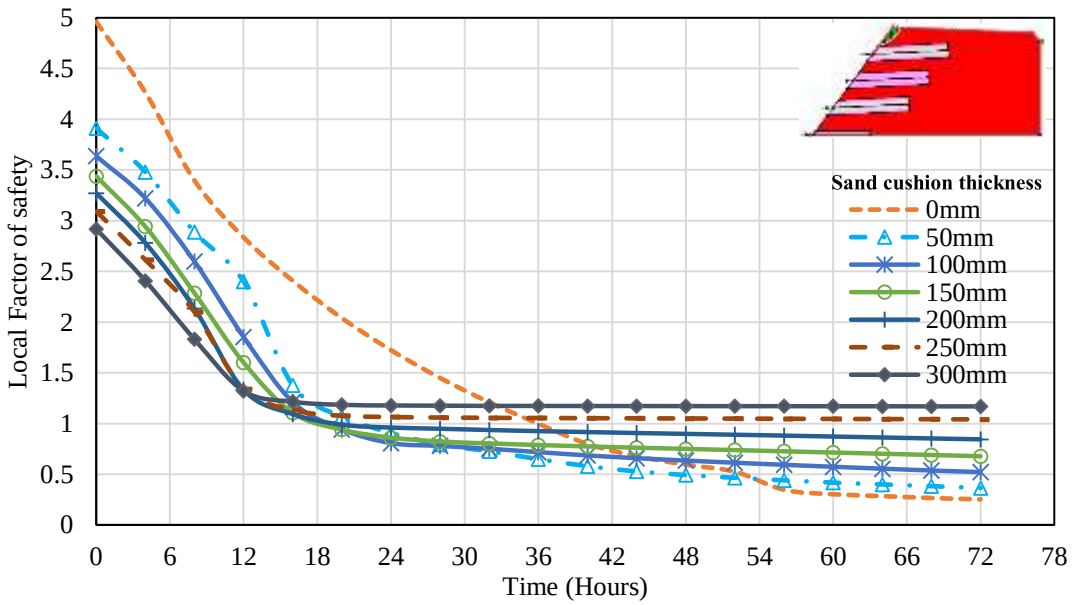

Figure 4.16: Local factors of safety of RCS embankments with varying sand cushion thickness.

Initially the factors of safety of the embankments with sand cushion decreased with increase in the sand cushion layer thickness. This as explained in the pore-water profile section is attributed to the initial matric suction of sand (-3.5kPa) and RCS (-60kPa). The lower matric suction value of sand was rapidly lost as the rainfall flux infiltrated through the RCS embankment contributing to lower factors of safety. Factors of safety of embankments are dependent on the shear strength of the soil and the reduction in the shear strength of the soil due to pore water pressure development ultimately contributed to the lower factor of safety in the embankment. However, at 18 hours the factors of safety curves of the different embankments with sand cushions converged. This marked the point at which most parts of the RCS above the top most geotextile layer became saturated. Due to the high volumetric water content in the RCS layers, the shear strength of the embankment was no longer dependent on the matric suction of the soils but was now largely dependent on the drainage and effective soil shear provided by the sand cushion layer. This explains the change in the curve trends after the convergence, with the embankments having thicker sand layers now recording the best trends in the local factors of safety of the embankments. The trend continued till the end of the rainfall event with the factors of safety of the embankments increasing with increase in the sand layers thickness. After a period of 30hours only sand layers of thickness 250mm and 300mm provided the required strength for the local stability of the embankment as marked by factors of safety above 1. This was maintained till the end of the three day rainfall event. it is thus determined that for the embankment to be safe against local failure, the top most geotextile layer has to be provided with a sand layer of thickness 250mm.

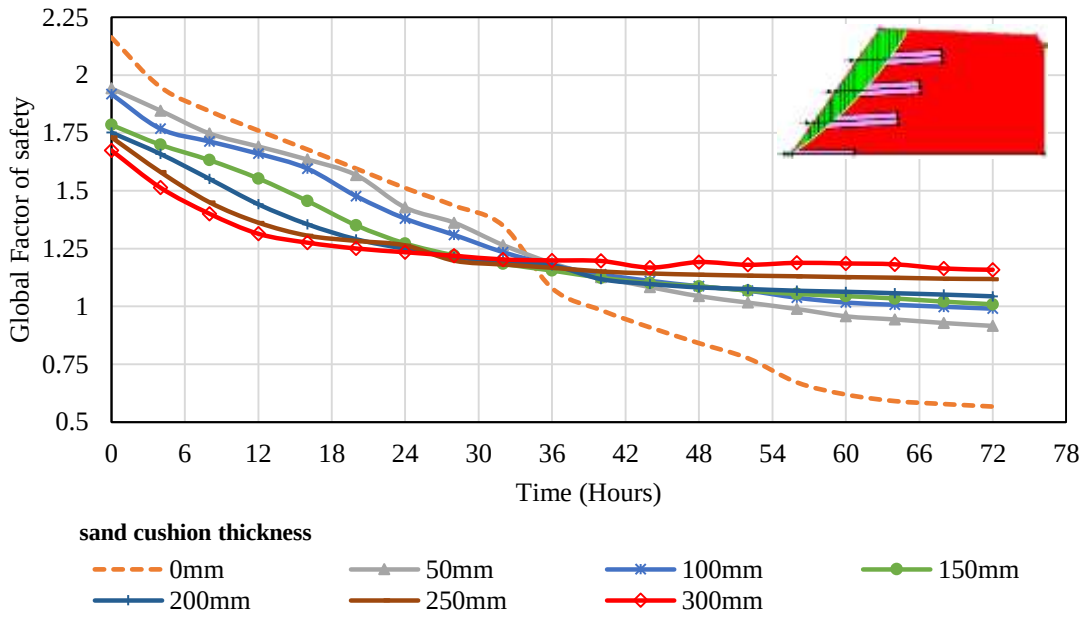

Figure 4.17: Local factors of safety of RCS embankments with varying sand cushion thickness.

Similar trend in the global factors of safety of the embankments as with the local factors of stability of the embankment were observed as shown in Figure 4.17. The RCS embankment with no sand cushion layer had a rapid decline in the factors of safety and failing at 38hours as evidenced by a factor of safety below 1 at 38 hours. The factor of safety curves of the non-geotextile layers provided with sand cushion layers converged at 26 hours and as in the local factors of safety, this is the time period at which the rainfall flux had passed through the embankment and the RCS in most section was saturated. The stability of the embankment was now dependent on the drainage ability and shear strength parameters of the river sand layers and not on the matric suction of the RCS zones. An introduction of a 50mm sand layer increased the 72hours factor of safety of the embankment from 0.567 to 0.916 signifying a 61% increase in the global factors of safety a further increase to 150mm sand cushion layer improved the factor of safety of the embankment to 1.01 a 78% increase in the factors of safety.

Figure 4.18 shows the contribution of sand layers thickness on the factors of safety of the geotextile reinforced embankment based on the end of third day results. Both the global and local factors of safety of the embankments increased with increase in sand layer thickness. A sand layer thickness of 100mm improved the global factor of safety of the RCS embankments from the unstable factor of 0.255 when without sand layers to the stable factor of safety of 1 on the third day of the rainfall event.

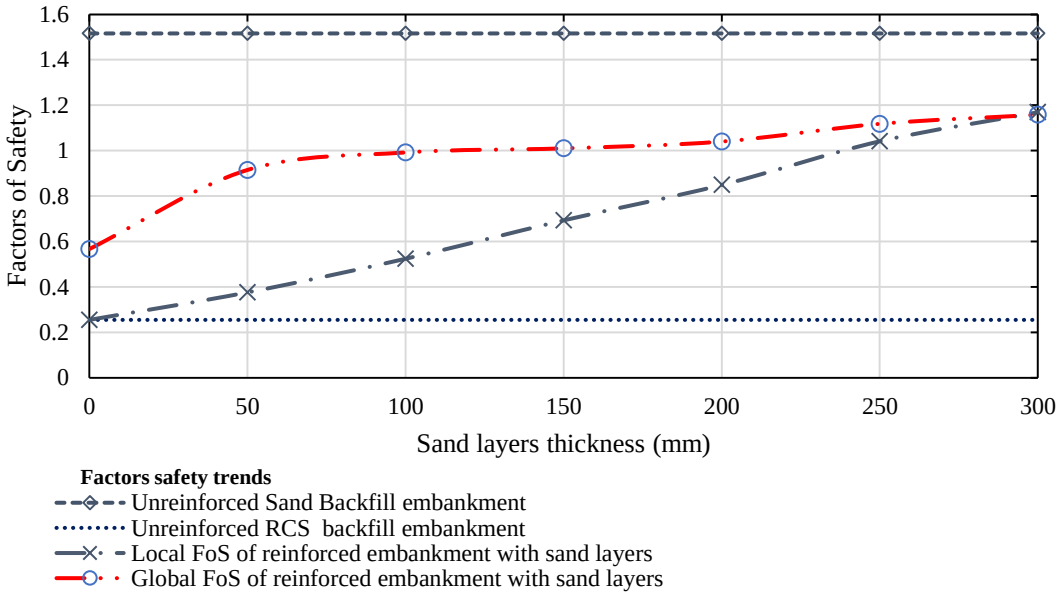

Figure 4.18: Contribution of sand layer thickness in the improvement of factors of safety of embankments

Results from the numerical simulation show that there is an improved stability in the embankment with increase in the sand layer thickness. Provision of sand layers above 100mm thick was found to improve on the stability of the embankment throughout the rainfall event. A sand layer thickness of 150mm was however determined in this study to be adequate in the improvement of the global stability of the embankment. A sand cushion layer of 150mm ultimately reduces the amount of sand required in the embankment construction to 15% and significantly improves the stability of the embankment subjected to rainfall event.

4.5 Effect of Drainage Layers Spacing on the Drainage and Stability of RCS Embankments

4.5.1 Pore-water pressure evaluation

Figure 4.19 presents pore water variations with change in drainage layer spacing. The sand cushion layer thickness of 150mm was adopted in this evaluation. From the Figure the pore-water profile of the embankment with 1m geotextile reinforcement spacing recorded the lowest pore-water pressure development at the end of day one with the embankment with drainage layers spaced at 0.25m recording the highest pore water pressure developments in its profiles. At the end of day one the embankment with 0.25m spaced drainage layers recorded very high levels of pore-water pressure within them. This was attributed to the increase in the sand medium channels through which rain water infiltrated into the RCS from the sloping end of the embankment in which the sand layers were exposed to the rainfall event. This contributed to the pore water pressures within the embankment to be the highest. However in the embankment with the drainage layers spaced at 1.0m intervals, the embankment could only accommodate two drainage layers located at an elevation of 1m and 2m vertical distance. With a reduced number of drainage layers and the poor hydraulic conductivity of the RCS the amount of water infiltrating into the embankment was reduced thus the lowest pore-water pressure levels within the embankment with drainage layer spaced at 1m interval at the end of day one.

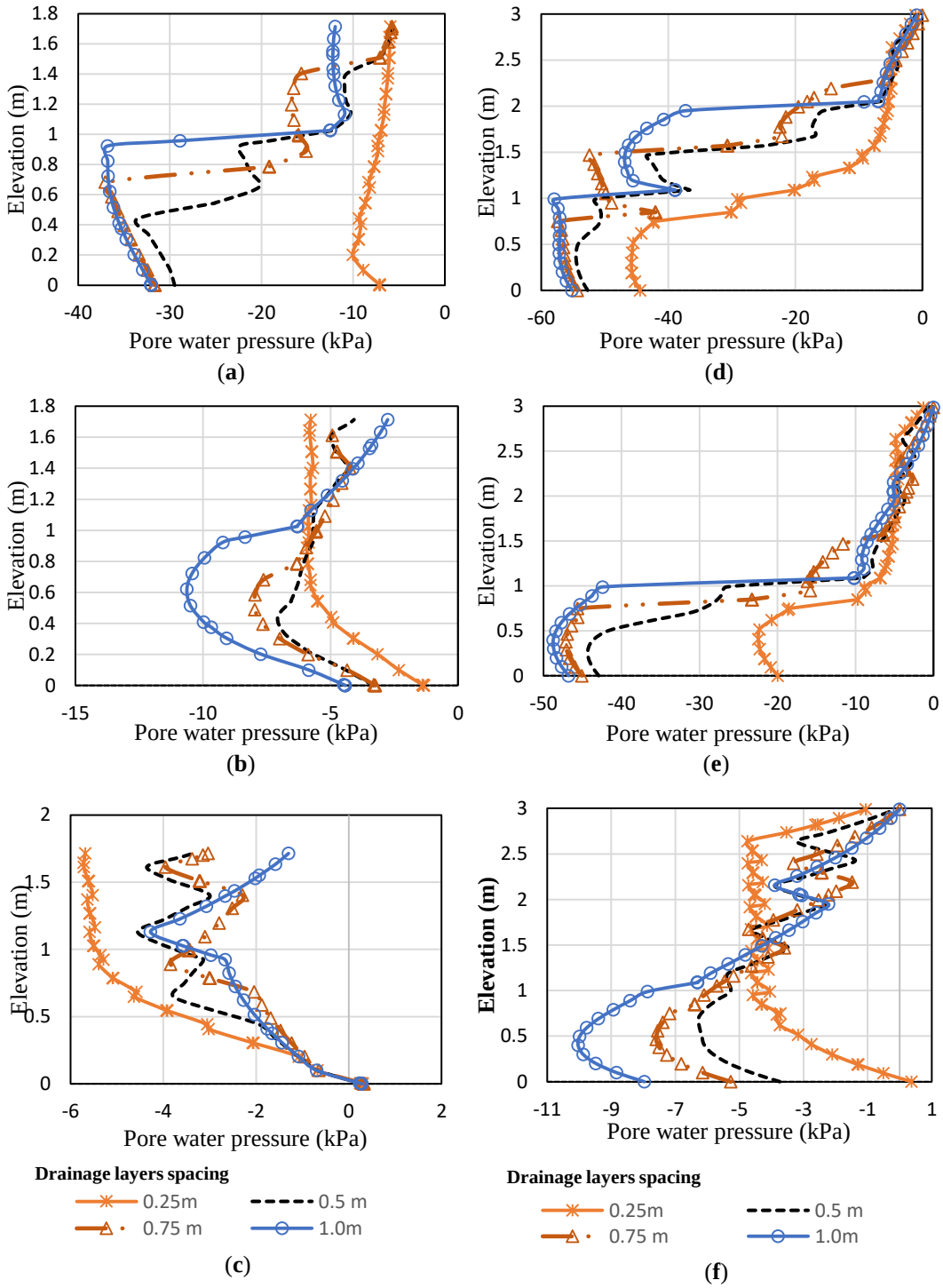

Figure 4.19: Pore-water profiles of embankments with change in drainage layer spacing at end of: (a) day one x=1.2m from toe; (b) day two x=1.2m; (c) day three x=1.2m; (d) day one x=2.4m from toe (e) day two x=2.4m and (f) day three x=2.4m.

Water entry into the embankment through many channels in the early stages contributed to the pore-pressure profiles of the 0.25m spaced drainage layers to be significantly high. This was partly aided by the low matric suction of the river sand and a significantly high hydraulic conductivity values as compared to the RCS. Embankments with 1m drainage layers spacing recorded very low pore-water pressure profiles in the initial stages due to the low hydraulic conductivity of the RCS. However with passage of time the infiltration flux managed to pass through the entire RCS embankment. As can be seen in day three, the pore-water pressure profiles of embankments with drainage layers spaced at 0.25m was the best while the pressure development in the 1m drainage layers spacing was the poorest. This is because the drainage layers were now performing draining functions which ultimately helped reduce the rate of pore water pressure build up. Embankments with many drainage layers which is characterised by small drainage layer spacing performed better with low pore-water pressure build up while their counterparts with 1m spaced drainage layers had a higher rate of pressure development due to poor drainage in the embankment.

Based on the numerical results reduction of the drainage layers spacing significantly improves the performance of the RCS embankments in long duration rainfall events as pore-water pressure is easily dissipated. Spacing of 0.75m and less adequately serves in improving drainage within the embankment with much smaller spacing of 0.25m recording the best performance in pore water pressure dissipation. The 0.5m spacing of drainage layer (composed of 150mm sand layer and non-woven geotextile) is thus determined to be adequate to address drainage in the RCS embankment.

4.5.2 Local and Global Stability

Figure 4.20 shows the local factors of safety of the embankment with change in drainage layer spacing. The drainage layer spacing affected the distance from the flat top of the embankment to the first drainage layer. Drainage layers spacing of 0.25m 0.5m resulted in the first drainage layer of the embankment to be located at a distance of 2.5m in elevation.

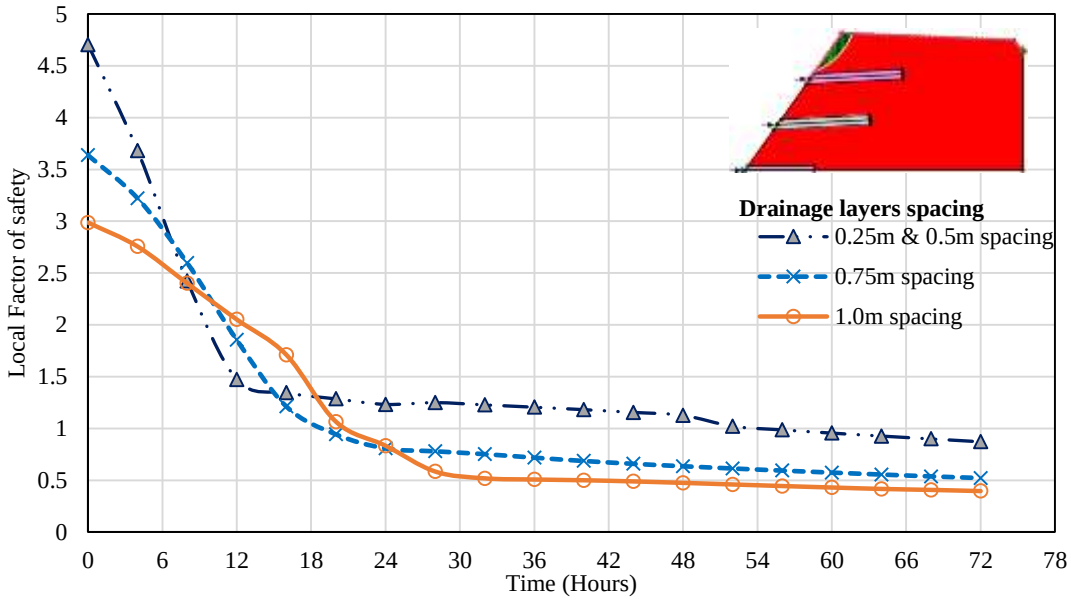

Figure 4.20: Local factors of safety of RCS embankments with varying sand cushion thickness

From the Figure drainage layer spacing of 1m recorded the poorest factors of safety in most session of the rainfall event while drainage layer spacing of 0.25and 0.5m recorded the best factors of safety trend. This is attributed to the depth of RCS above drainage layer. At a drainage spacing of 1m the top most drainage layer was located at an elevation of 2.0m, this ultimately left a RCS layer of 0.85m to the top of the embankment. In the 0.25m and 0.5m drainage layer spacing the depth of the RCS is reduced to 0.35m to the top of the embankment. Large depths of RCS above the drainage layers led to the accumulation of infiltrating water within the RCS zone due to low hydraulic conductivity of the RCS. Accumulation of the infiltrating water

contributed to the development of pore-water pressure within the RCS zone ultimately leading to reduced shear strength of the RCS thus lowering factors of safety. The drainage layer spacing of 0.5m and 0.25m offered the required strength for the stability of the embankment throughout the rainfall event. A spacing of 1.0m in the drainage layers will expose the embankments to local failure at 20 hours of continuous rainfall event. Trends in the global factors of safety of the RCS embankment are as shown in Figure 4.21.

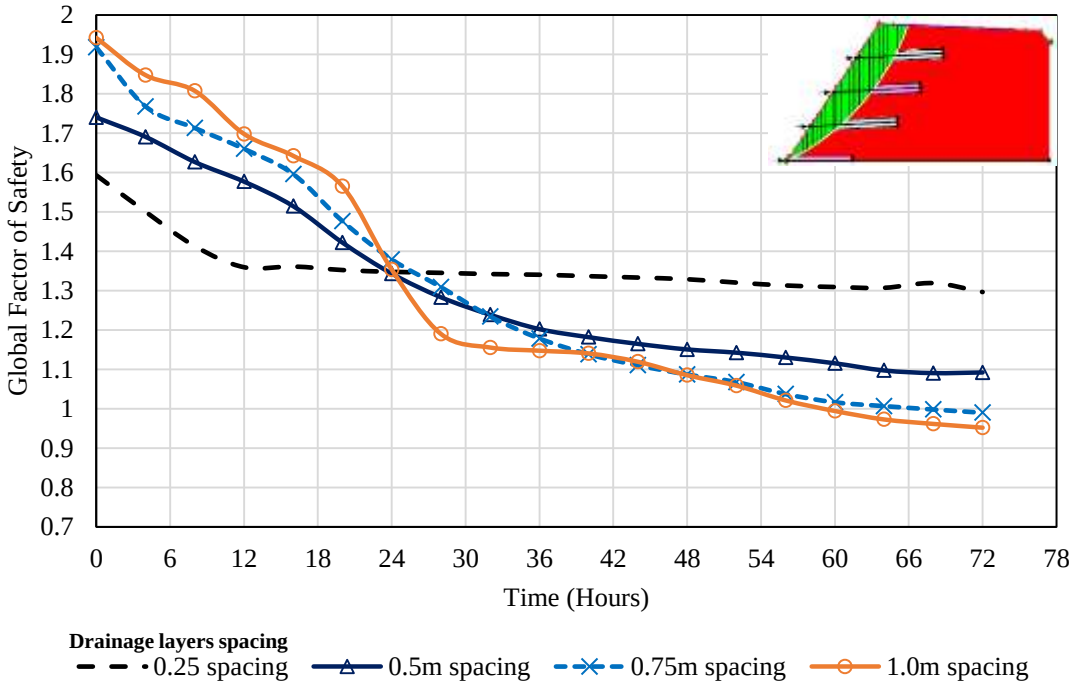

Figure 4.21: Global factors of safety of RCS embankments with varying sand cushion thickness

Figure 4.21 presents the variation of global factors of safety with change in drainage layer spacing. Spacing of geotextiles and drainage layer in the RCS is observed to have an impact on the stability of the embankment. Unlike in the local factors of safety where 0.25m drainage spacing recorded the best factors of safety in most parts of the rainfall event the trend in the global factors of safety were different. Corresponding to initial low pore-water pressure values in its pore-water pressure profile, the

embankments with 1.0m drainage layers spacing in the initial stages had high factors of safety values. This was because of the low hydraulic conductivity of the RCS which made the rate of the infiltrating water flux to take long in its movement within the RCS zones. However, with change in time the embankments with 0.25m spaced drainage layers recorded far better factors of safety. As earlier explained this is attributed to the ingress of water in the embankment with the sand layers serving as transmission medium. When the volumetric water content became high in the embankment, embankments with closely spaced drainage layers had better drainage within them thus pore-water pressure accumulation was at a lower rate as compared to those with larger spacing. The soil shear strength is dependent on the pore-water pressure of the soil. High pore-water pressure in the embankments leads to lower shear strength in the soil hence, in the latter stages lower factors of safety of safety were recorded for the embankments with large drainage layers spacing. With proper drainage in the embankments with 0.25m spaced drainage layers pore-water dissipation was much better thus improved shear strength of the soil and consequently improved factors of safety.

From the numerical results closely spaced drainage layers improved the performance of RCS. Closely spaced drainage layers also presented the advantage of the factor of stability of the embankments having minimal variations through the rainfall event as evidenced by the 0.25m drainage layers spacing which maintained factors of safety above 1.3 throughout the rainfall event. On the other hand the embankment with drainage layer spacing of 1.0m had a rapid decline in its factors of safety attributed to the poor drainage in the embankment and ultimate failure was observed after 60 hours

with the 0.75m drainage spacing layers failing after 66 hours. However the 0.5m drainage layer spacing maintained the stability of the embankment throughout the rainfall event and was thus determined to be adequate in improving the stability of the embankment as the factor of safety is way above one, a factor below which failure of the embankment is imminent.

CHAPTER FIVE

CONCLUSIONS AND RECOMMENDATIONS

5.1 Conclusions

This study evaluated the performance of RCS as an alternative backfill material in the construction of embankments. The performance of the RCS embankments under different drainage conditions was evaluated. The findings of the study demonstrated a great potential of RCS as backfill materials in embankment structures. Specifically the study concluded that;

i. Numerical model SEEP/W is suitable in predicting infiltration within unsaturated soil with a coefficient of determination of 0.828 arrived at in this study. Quadrilateral elements are the best in predicting infiltration in unsaturated soils and recorded higher values of coefficient of determination.

ii. Inclining non-woven geotextile layers makes them drain water much earlier than when not inclined and an optimum inclination angle of 3 degrees determined to be effective in the improvement of drainage and stability of RCS embankments. Any increase in the angle of inclination beyond three degrees does not offer any significant improvement on the performance of RCS embankments.

iii. Inclusion of sand layers provide both drainage and strength functions thus improve on the performance of RCS embankments. Provision of sand layers improved on the drainage of the RCS embankments. The stability of the embankments increases with increase in sand cushion layer thickness. A sand cushion thickness layer of

150mm is determined to be adequate in the improvement of RCS embankments performance.

iv. Drainage layer spacing contributes to the pore-water pressure development and stability in RCS embankments. Closely spaced drainage layers improves the drainage and stability of RCS embankments for long duration rainfall events. Drainage layer spacing of 0.5m was determined to be adequate in the drainage and stability of RCS embankments.

5.2 Recommendations

In order to conserve the environment, and cut costs in the construction of embankments, RCS can be safely used by provision of drainage layers composed of nonwoven geotextiles sandwiched between layers of 150mm river sand with the drainage layers inclined at three degrees above the horizontal.

5.2.1 Further studies

The current study focused on the pore water and stability performance of the RCS embankments with sand cushion layers. There was an improvement on the performance of the RCS embankments however, further studies are recommended;

i. To establish the deformations in the RCS embankments during rainfall infiltrations.

ii. To determine the performance of various other marginal soils available in construction sites, as this research investigated only the red coffee soils sourced from Juja, Kenya.

REFERENCES

Abdi, M. ., & Zandieh, A. . (2014). Experimental and Numerical Analysis of Large Scale Pullout Tests Conducted on Clays Reinforced with Geogrids Encapsulated with Coarse Material. Geotextiles and Geomembranes. *Geotextile and Geomembranes*, *42*(5), 494–504.

Albino, U. da R., & Portelinha, F. H. M. (2017). Numerical modeling of 1D infiltration on unsaturated interfaces between soil and geosynthetics. In *Proceedings of the 19th International Conference on Soil Mechanics and Geotechnical Engineering, Seoul 2017* (pp. 885–888).

Ashraf, M., & Ismail, M. (2012). Stability Analysis of Kelau Earth-Fill Dam Design under Main Critical Conditions. *Engineering Journal and Geotechnical Engineering*, 3209–3219.

ASTM D2487. (2017). *Standard Practice for Classification of Soils for Engineering Purposes (Unified Soil Classification System)*. ASTM International, West Conshohocken, PA, USA.

ASTM D3080. (2011). *Standard Test Method for Direct Shear Test of Soils Under Consolidated Drained Conditions*. ASTM International, West Conshohocken, PA, USA.

ASTM D4318. (2017). *Standard Test Methods for Liquid Limit, Plastic Limit, and Plasticity Index of Soils*. ASTM International, West Conshohocken, PA, USA.

ASTM D4643. (2017). *Standard Test Method for Determination of Water Content of Soil and Rock by Microwave Oven Heating*. ASTM International, West Conshohocken, PA, USA.

ASTM D4767. (2011). *Standard Test Method for Consolidated Undrained Triaxial Compression Test for Cohesive Soils*. ASTM International, West Conshohocken, PA, USA.

ASTM D6913. (2017). *Standard Test Methods for Particle-Size Distribution (Gradation) of Soils Using Sieve Analysis*. ASTM International, West Conshohocken, PA, USA.

ASTM D698. (2012). *Standard Test Methods for Laboratory Compaction Characteristics of Soil Using Standard Effort (12 400 ft-lbf/ft3 (600 kN-m/m3))*. ASTM International, West Conshohocken, PA, USA.

ASTM D7928. (2017). *Standard Test Method for Particle-Size Distribution (Gradation) of Fine-Grained Soils Using the Sedimentation (Hydrometer) Analysis*. ASTM International, West Conshohocken, PA, USA.

ASTM D854. (2014). *Standard Test Methods for Specific Gravity of Soil Solids by Water Pycnometer*. ASTM International, West Conshohocken, PA, USA.

Berg, R. R., Christopher, B. R., & Samtan, N. C. (2009). *Design and Construction of Mechanically Stabilized Earth Walls and Reinforced Soil Slopes* (FHWA-NHI-1). Washington, DC: U.S. Department of Transportation Federal Highway Administration.

Choudhary, K. A., & Krishna, M. A. (2016). Experimental Investigation of Interface Behaviour of Different Types of Granular Soil / Geosynthetics. *International Journal of Geosynthetics and Ground Engineering*, *2*(4), 1–11.

Christopher, B. R., & Stulgis, R. P. (2005). *Low Permeable Backfill Soils in Geosynthetic Reinforced Soil Walls: State of the Practice in North America*.

Denge, S. M. (2017). The Effect of Quarry Dust Concrete and Underlying Sub-Soil Medium on the Structural Performance of Dwelling House Ground Floors. *IOSR Journal of Mechanical and Civil Engineering*, *14*(02), 52–56. https://doi.org/10.9790/1684-1402035256

Fredlund, D. G. (2006). Unsaturated Soil Mechanics in Engineering Practice. *Journal of Geotechnical and Geoenvironment Engineering*, (March), 286–321.

García-aristizábal, E. F., Vega-posada, C. A., & Gallego-hernández, A. N. (2016). Experimental study of water infiltration on an unsaturated soil-geosynthetic system. *Revista Facultad de Ingeniería, Universidad de Antioquia*, (78), 112–118.

Garcia, E. F., Gallage, C. P. K., & Uchimura, T. (2007). Function of permeable geosynthetics in unsaturated embankments subjected to rainfall infiltration. *Geosynthetics International*, *14*(2), 89–99.

GEO-SLOPE International. (2010). *Seepage Modeling with SEEP / W 2007*. *Geostudio Helpfile*. Calgary,Canada.

Iryo, T., & Rowe, R. K. (2003). On the Hydraulic Behavior of Unsaturated Nonwoven

Geotextiles. *Geotextiles and Geomembranes*, *21*(2003), 381–404.

Iryo, T., & Rowe, R. K. (2005). Infiltration into an embankment reinforced by nonwoven geotextiles. *Canadian Geotechnical Journal*, *42*, 1145–1159.

Khire, M. V, Benson, C. H., & Bosscher, P. J. (2000). Capillary Barriers:Design Variables and Water Balance. *Journal of Geotechnical and Geoenvironment Engineering*, *126*(August), 695–708.

Koerner, R. M., & Koerner, G. R. (2013). Geotextiles and Geomembranes A data base , statistics and recommendations regarding 171 failed geosynthetic reinforced mechanically stabilized earth (MSE) walls. *Geotextiles and Geomembranes*, *40*, 20–27.

Lin, C., & Yang, K.-H. (2014). Experimental Study on Measures for Improving the Drainage Efficiency of Low-Permeability and Low-Plasticity Silt with Nonwoven Geotextile Drains. *Journal of the Chinese Institute of Civil and Hydraulic Engineering*, *26*(2), 71–82.

Lu, N., Godt, J. W., & Wu, D. T. (2010). A closed form equation for effective stress in unsaturated soil. *Water Resources Research*, *46*, 1–14.

Lu, N., & Likos, W. J. (2004). *Unsaturated Soil Mechanics*. New York: John Willey & Sons, Inc.

Lu, N., & Likos, W. J. (2006). Suction Stress Characteristic Curve for Unsaturated Soil. *Journal of Geotechnical and Geoenvironment Engineering*, (February), 131–142.

Maula, B. H., & Zhang, L. (2011). Assessment of Embankment Factor Safety Using Two Commercially Available Programs in Slope Stability Analysis. In *The Twelfth East Asia-Pacific Conference on Structural Engineering and Construction* (pp. 559–566). https://doi.org/10.1016/j.proeng.2011.07.070

Mccartney, J. S. (2007). *Determination of the Hydraulic Characteristics of Unsaturated Soils Using a Centrifuge Permeameter*. The University of Texas at Austin.

Morgenstern, N. R. (1979). Properties of Compacted Soil. In *Contribution to panel discusion, Section IV, 6th Panamerican Conference on Soil Mechanics and Foundation Engineeirng, Vol. 3* (pp. 349–354).

Murad, A.-F., Coronel, J., & Tao, M. (2007). Effect of Soil Moisture Content and Dry Density on Cohesive Soil – Geosynthetic Interactions Using Large Direct Shear Tests. *Journal of Materials In Civil Engineering*, *19*(7), 540–549.

Nishigaki, M., Umeda, & Kono. (1993). A study of function ofgeofilters spread in compacted soil embankment. In *Proceedings of the Symposium on investigation, Design and construction for Unsaturated ground, The Japanese Geotechnical society* (pp. 135–138).

Njike, M., Oyawa, W., & Nyomboi, T. (2014). Effect of Hand Compaction on Compressive Strength and Water Absorption of Compressed Stabilized Earth Blocks. *International Journal of Structural and Cvil Engineering Research*, *3*(3), 116–132.

Patricia, W. M. (2015). *Environmental and Socio-Economic Impacts of Sand Harvesting On the Community In River Kivou Catchment, Mwingi Sub County, Kitui County, Kenya. Masters of Science*. Kenyatta University,Nairobi Kenya.

Raisinghani, D. V, & Viswanadham, B. V. S. (2010). Geotextiles and Geomembranes Evaluation of permeability characteristics of a geosynthetic-reinforced soil through laboratory tests. *Geotextiles and Geomembranes*, *28*(6), 579–588. https://doi.org/10.1016/j.geotexmem.2010.01.001

Raisinghani, D. V, & Viswanadham, B. V. S. (2011). Centrifuge model study on low permeable slope reinforced by hybrid geosynthetics. *Geotextiles and Geomembranes Journal*, *29*, 567–580.

Shukla, S. K., Sivakugan, N., & Das, B. M. (2011). A state-of-the-art review of geosynthetic- reinforced slopes, 17–32. https://doi.org/10.3328/IJGE.2011.05.01.17-32

Thuo, J. N., Huynh, V. D. A., Yang, K., & Portelinha, F. H. M. (2016). Behavior of Geotextile / Geogrid Reinforced Slopes with Various Backfills subject to Rainfalls, (November), 1–10.

Thuo, J. N., Yang, K. H., & Huang, C. C. (2015). Infiltration into unsaturated reinforced slopes with nonwoven geotextile drains sandwiched in sand layers. *Geosynthetics International*, *22*(6), 457–474.

Tolooiyan, A., Abustan, I., Selamat, M. R., & Ghaffari, S. (2009). A Comprensive Method

for Analyzing the Effect of Geotextile Layers on Embankment Stability. *Geotextiles and Geomembranes*, *27*, 399–405.

Vanapalli, S. K., Fredlund, D. G., Pufahl, D. ., & Cliffton, A. . (1996). Model for the prediction of shear strength with respect to soil suction.pdf. *Canadian Geotechnical Journal*, *33*, 379–392.

Wu, J., Chou, & Tang, A. (2010). Forensic Studies of ReinforcedSlope Failure in Taiwan. In *The 1st International GSI-Asia Geosynthetics Conference, Taichung, Taiwan* (pp. 185–188).

Xue, K., Ajmera, B., Tiwari, B., & Hu, Y. (2016). Effect of long duration rainstorm on stability of Red-clay slopes. *Geoenvironmental Disasters*, *3*(12), 1–13. https://doi.org/10.1186/s40677-016-0046-9

Yang, K. H., Thuo, J. N. ang'a, Huynh, V. D. A., Nguyen, T. S., & Portelinha, F. H. M. (2017). Numerical evaluation of reinforced slopes with various backfill-reinforcement-drainage systems subject to rainfall infiltration. *Computers and Geotechnics*, *96*(April), 25–39. https://doi.org/10.1016/j.compgeo.2017.10.012

Yoo, C., & Jung, H. (2006). Case History of Geosynthetic Reinforced Segmental Retaining Wall Failure. *Journal of Geotechnical and Geoenvironment Engineering*, *132*(12), 1538–1548.

Zhang, L. L., Fredlund, D. G., Fredlund, M. D., & Wilson, G. W. (2014). Modeling the unsaturated soil zone in slope stability analysis. *Canadian Geotechnical Journal*,

(December).

Zornberg, J. G., Bouazza, A., & Mccartney, J. S. (2010). Geosynthetic capillary barriers : current state of knowledge. *Geosynthetics International*, *17*(5), 273–300.